THE PRECIPITATE EVOLUTION IN THE NICKEL-BASED SUPERALLOY IN738LC

by

Dinç Erdeniz

B.S., Mechanical Engineering, Ege University, 2005

Submitted to the Institute for Graduate Studies in
Science and Engineering in partial fulfillment of
the requirements for the degree of
Master of Science

Graduate Program in Mechanical Engineering

Boğaziçi University

2008

ACKNOWLEDGEMENTS

I would like to thank my advisor Assistant Professor Ercan Balıkçı for his guidance and constant support during the preparation of this thesis. I am very fortunate to have the opportunity to work with him. I would also like to thank my thesis committee members, Assistant Professor Nuri Ersoy and Professor Turan Özturan, for their valuable advice and suggestions. My sincere gratitude goes to Professor Teiichi Ando of the Mechanical and Industrial Engineering Department at Northeastern University, for his continuous support and patience.

I am very proud of working with many talented people in the Department of Mechanical Engineering at Boğaziçi University. I would like to express my sincere appreciation to all my colleagues for their help and friendship. I am also thankful to all members of Boğaziçi University Advanced Technologies R&D Center, especially Ms. Ayşe Çetin, Dr. Bilge Gedik Uluocak, and Ms. Aslı Çakır Saygılı, for their help with the metallography and scanning electron microscopy.

I would like to thank my parents Tunç Erdeniz and Nedret Erdeniz, my sister Zeren Gürsoy, my brother Burç Erdeniz, and my brother-in-law Ender Gürsoy for their constant encouragement and support during my education at Boğaziçi University. My graceful prayers go to my dear grandmother Şehber Erdeniz, who deceased in November 2007, before the completion of this study. I know that life will be tougher without her support.

This work was funded by Boğaziçi University Scientific Research Projects (BAP) under the grant # 05HA601.

ABSTRACT

THE PRECIPITATE EVOLUTION IN THE NICKEL-BASED SUPERALLOY IN738LC

IN738LC is a polycrystalline, nickel-based superalloy, which is widely utilized in a variety of aggressive applications such as those experienced in jet engines, land-base gas turbines, and high temperature catalytic reactors. This material provides high performance in aggressive environments at temperatures above 650°C. The expected properties at these temperatures are corrosion resistance, optimal thermal properties, creep and fatigue resistance, and optimal impact and wear resistance. These required properties are obtained via solid solution hardening and precipitation hardening of face-centered cubic (FCC) nickel (Ni) matrix phase. Precipitates in the Ni-base superalloys are generally in the form of ordered Ni_3Al intermetallic compounds. The size, morphology, and distribution of these precipitates determine the properties of the material. Thus, microstructure control and stabilization is very important for effective use of IN738LC.

In this study, a number of heat treatments are employed for observation of the life cycle of a precipitate, which starts with nucleation, continues with growth, and ends with dissolution. First part of this thesis explores the formation of cooling precipitates. In the second part, formation of duplex-size microstructure at 1140°C is studied. Coarsening and dissolution mechanisms are discussed in the third part for the data obtained from heat treatments at 1120°C for 12-480 hours. These treatments have given the chance to observe agglomeration of precipitates. Growth features of both fine and coarse precipitates under actual thermal conditions are studied in the fourth part. Heat treatments are conducted at 950°C for 1-480 hours. The results have showed that fine precipitates grow faster than coarse ones at this temperature, but 480 hours are not sufficient to obtain a unimodal precipitate microstructure.

ÖZET

NİKEL BAZLI SÜPERALAŞIM IN738LC'DE ÇÖKELTİ GELİŞİMİ

IN738LC çok taneli, nikel bazlı bir süperalaşımdır. Uçak motorlarında, gaz türbinlerinde ve yüksek sıcaklık katalitik reaktörlerde yaygın olarak kullanılmaktadır. 650°C üzerinde ve malzemeyi yıpratacak özellikteki atmosferlerde yüksek performans göstermektedir. Korozyon dayanımı, optimum ısıl özellikler, sürünme ve yorulma dayanımı, darbe ve aşınmaya karşı optimum dayanım bu malzemeden beklenen bazı özelliklerdir. Bu özellikler katı çözelti sertleşmesi ve çökelti sertleşmesi yöntemleriyle yüzey merkezli kübik (YMK) nikel (Ni) matris fazının güçlendirilmesi yoluyla elde edilmektedir. Çökeltilerin boyutu, şekli ve dağılımı malzeme özelliklerini tayin etmektedir. Bu nedenle, içyapı kontrolü malzemenin etkin bir şekilde kullanılması açısından son derece önemlidir.

Bu çalışmada, çökeltilerin gelişimini gözlemek adına bazı ısıl işlemler tatbik edilmiştir. İlk bölümde, soğuma çökeltilerinin oluşumu incelenmiştir. İkinci bölümde, 1140°C'de iki farklı boyutta çökeltilerin oluşumu gözlenmiştir. 1120°C'de 12-480 saat arasında uygulanan ısıl işlemlerin ışığında, çökeltilerin büyüme ve çözünme mekanizmaları bu çalışmanın üçüncü bölümünde ele alınmıştır. Bu işlemler çökelti birleşme mekanizmasının da gözlemlenmesine olanak tanımıştır. Dördüncü bölümde, büyük ve küçük çökeltilerin gerçek ısıl koşullar altındaki büyüme nitelikleri üzerinde durulmuştur. Isıl işlemler 950°C'de 1-480 saat arasında uygulanmıştır. Sonuçlar, küçük çökeltilerin daha hızlı büyüdüğünü, ancak 480 saatin tek boyutlu bir çökelti içyapısı elde etmek için yeterli olmadığını göstermiştir.

TABLE OF CONTENTS

LIST OF FIGURES

LIST OF TABLES

LIST OF SYMBOLS/ABBREVIATIONS

A	Interfacial area
d_0 , d_t	Particle size
d_γ , $d_{\gamma'}$	Unstressed interplanar spacings of matrix and precipitate phases
ΔG_{hom}	Total free energy change associated with homogeneous nucleation
ΔG_{het}	Total free energy change associated with heterogeneous nucleation
ΔG_d	Free energy associated with an eliminated defect
ΔG_s	Free energy associated with the misfit strain
ΔG_v	Free energy associated with the formation of a volume
K	Rate constant
n	Growth exponent
Q	Molar activation energy
r	Radius of a spheroid
R	Universal gas constant
t	Time
T	Absolute temperature
T_m	Melting Temperature
V	Volume
Γ	Interfacial energy
δ	Lattice misfit
APB	Anti-phase boundary
BCC	Body-centered cubic
BSE	Back scattered electron
FC	Furnace cooling
FCC	Face-centered cubic
FEG	Field emission gun
HIP	Hot isostatic pressing

PAM	Precipitate agglomeration mechanism
SEM	Scanning electron microscopy
TCP	Topologically close-packed
TEM	Transmission electron microscopy
WQ	Water quenching

1. INTRODUCTION

1.1. General

Superalloys are a group of high temperature materials which are utilized in applications, especially for jet engines, nuclear reactors, and land-base gas turbines [1, 2]. A few attractive properties of these materials for such applications are high strength at high temperatures, resistance to corrosion, excellent creep and fatigue resistance, and metallurgical stability above 650°C [3]. They are composed of about a dozen of elements. In general, they have a nickel-, cobalt-, or iron-base matrix; also a combination of nickel-iron matrix is possible. Superalloys are strengthened primarily by solid solution hardening, precipitation of an intermetallic phase, and carbides especially in cobalt-base grades [4].

First studies reported on superalloys were in the 1930s, which aimed at responding the need for more heat resistant materials in aircraft engine turbo superchargers [1]. In the course of time, aircraft engines have reached higher temperatures in order to increase efficiency, thus superalloy researches have accelerated. Today, superalloys are the most dominantly used materials for aircraft engines, especially components which are subjected to loading at high temperatures and aggressive environments. A wide range of superalloys have been employed for various service conditions [5], and they are still being improved parallel to the development of engine technology.

Nickel-base superalloys are the most commonly used of all superalloys and metallurgically the most complex materials of any alloys [6]. They approximately constitute 50 per cent of an advanced aircraft engine [1]. As a matrix material, face-centered cubic (FCC) nickel has the advantage of the high phase stability and capability to be strengthened by various processes [3].

Cobalt-base superalloys maintain their second place in the gas turbine industry. They are chemically much less complex than nickel-base superalloys. They are strengthened chiefly by precipitation of metal carbides. These materials have the advantage

of superior hot corrosion resistance due to high chromium contents. They also exhibit better thermal fatigue resistance and weldability in comparison to nickel-base superalloys [2]. But they tend to precipitate undesirable phases, such as σ, Laves, and similar topologically close packed (TCP) phases [3].

Iron-base superalloys have evolved from an austenitic stainless steel (close packed FCC structure) matrix and are strengthened by both solution hardening and precipitate forming elements. The matrix is, sometimes, alloyed with at least 25 per cent Ni to stabilize the FCC phase; this type of alloys are named as nickel-iron-base superalloys. The precipitates are generally ordered intermetallics, such as Ni_3Al (γ′), Ni_3Ti (η), Ni_3Nb (γ″) [3].

Superalloys are generally strengthened by precipitation hardening and solid solution strengthening. In precipitation hardening, ordered intermetallic particles block the dislocation motion, which causes strengthening. The precipitates also impart coherency strains, which are formed because of the differences in lattice parameters of the matrix and particle phases. Presence of coherency strains is very important for effective strengthening of superalloys.

Since there are more than a dozen of elements in a superalloy, there are a number of phases other than precipitate phase, namely TCP phases, carbide phases, etc. TCP phases are generally unwanted in the microstructure, since they degrade the properties. Carbide phases may be useful in some cases. Some information will be given in the following sections.

In this thesis, precipitate evolution in a Ni-base superalloys is presented. The material used in the experimental part is, IN738LC, which is a Ni-base, polycrystalline superalloy. Experimental procedure is described in the second part of this thesis. In the third part, results analyzing precipitate microstructure evolution are given and discussed involving cooling precipitates, growth characteristics, coarsening behavior, and dissolution mechanism.

1.2. Literature Review

1.2.1. Metallurgy of Nickel-Base Superalloys

As stated earlier, Ni-base superalloys have very complex microstructural features, which are still attractive research topics. They generally constitute of about a dozen of elements, and all of these alloying elements influence several properties. These elements form a number of phases, some of them, like γ′ and γ″, are helpful in obtaining high performance properties, but some of them which are called TCP phases, like σ ($(Cr,Mo)_x(Ni,Co)_y$), μ (Mo_6Ni_7), and Laves ($Fe_{36}Cr_{12}Mo_{10}$), cause degradation of properties. Thus, it is extremely important to avoid formation of TCP phases, therefore chemical composition and microstructural stability of the alloy should be controlled accurately. Role of the alloying elements and effects of the phases on properties are discussed in this section.

1.2.1.1. Role of the Alloying Elements in Nickel Base Superalloys. Nickel base superalloys incorporate, about a dozen of elements (see Figure 1.1), like nickel, chromium, aluminum, titanium, and also tramp elements (the elements which find their way accidentally into the melt during production), like silicon, sulfur, oxygen, and nitrogen. Very small amounts of trace elements (the elements which exists inside the material with a very low amount), such as selenium, tellurium, lead, bismuth are also included. Material properties are strongly dependent on the composition and metallurgical stability; therefore, amounts of constituents must be controlled precisely. The roles of contributing elements in Ni-base superalloys were reviewed by Jena and Chaturvedi [7], and another review is concerned with the effects of trace and tramp elements on the properties of Ni-base superalloys by Holt and Wallace [8]. Those elements are generally classified into solid solution formers, precipitate formers, carbide formers, and surface stabilizers. Functions of some alloying elements in nickel-base alloys are given in Table 1.1 and compositions of representative nickel-base superalloys are listed in Table 1.2.

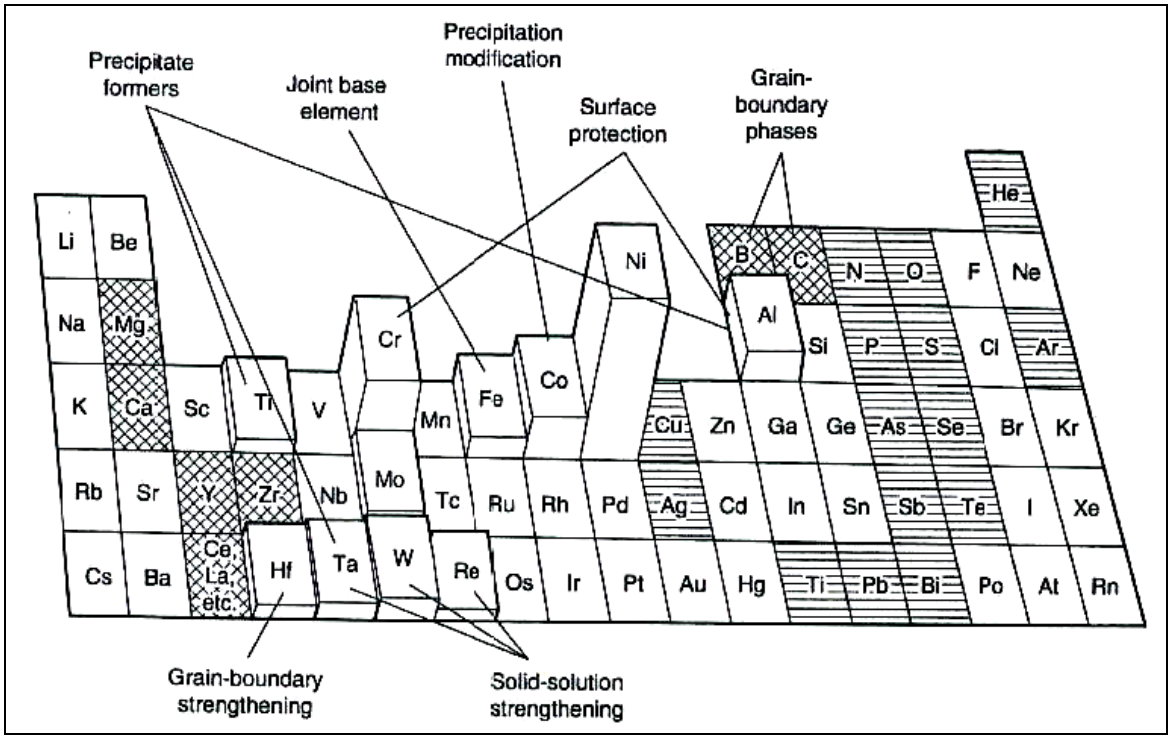

Figure 1.1. Alloying elements used in nickel base superalloys. Beneficial trace elements are marked with cross hatching and harmful trace elements are marked with horizontal line hatching [3].

Solid solution formers primarily increase the strength of matrix phase via retarding the dislocation motion. Solute atoms induce distortions in the lattice, then the slip of dislocations become harder. Carbides that form along the grain boundaries provide superior creep properties, since they prevent grain boundary sliding and migration. However, thin film grain boundary carbides are detrimental. The most common carbide types in Ni-base superalloys are MC, $M_{23}C_6$, M_7C_3, M_6C, where M represents metallic elements, such as W, Ta, Mo, Cr, Nb. Fine sized, dispersed metal carbides may also serve to strengthen the matrix [3].

External and internal surface stabilization are very crucial to prevent material degradation, which can be caused by oxidation and hot corrosion in aggressive environments. The presence of elements, like Cr, Al, Co, and La, is necessary for external surface stability. On the other hand, particles of $M_{23}C_6$ carbides help to stabilize internal surfaces, primarily grain boundaries. Also presence of elements, such as B, C, Zr, and Hf, contribute to strengthen the grain boundaries [7].

Table 1.1. Roles of elements in Ni-base superalloys [3]

Effect		**Elements**
Solid solution strengtheners		Co, Cr, Mo, W, Ta, Re
Carbide formers	MC	W, Ta, Ti, Mo, Nb, Hf
	M_7C_3	Cr
	$M_{23}C_6$	Cr, Mo, W
	M_6C	Mo, W, Nb
Carbonitrides: M(CN)		C, N
Forms γ′ Ni_3(Al, Ti)		Al, Ti
Raises solvus temperature of γ′		Co
Hardening precipitates and/or intermetallics		Al, Ti, Nb
Oxidation resistance		Al, Cr, Y, La, Ce
Improve hot corrosion resistance		La, Th
Sulfidation resistance		Cr, Co, Si
Improves creep properties		B, Ta
Increases rupture strength		B
Grain-boundary refiners		B, C, Zr, Hf

1.2.1.2. Phases Present in Nickel Base Superalloys. A number of reviews have been published about the microstructure of nickel-base superalloys [9-11]. They generally deal with the phases present in the alloy and their effects on the properties of material. Reactions of phases are also emphasized in these studies, for example carbide reactions. In this section, major phases present in a nickel-base superalloy are cited; their constitution and structure are analyzed. As mentioned earlier, Ni-base alloys are metallurgically the most complex of any alloys because of their chemically dynamic structures. Hence, influence of phases on properties and reactions of phases are summarized in this part.

The microstructure of a nickel-base superalloy is generally composed of a continuous nickel matrix phase (γ: Ni, Cr, Co, W, etc.) that contains substitutional solid solution elements, uniformly distributed precipitate phase (γ': Ni_3(Al,Ti,Nb)), different forms of metal carbide phases (MC, $M_{23}C_6$, M_7C_3), and some other minor phases, like borides and TCP phases.

Table 1.2. Chemical compositions of representative nickel base superalloys [2]

Alloy (wt.%)	Ni	Cr	Co	Mo	W	Ta	Cb	Al	Ti	Fe	Mn	Si	C	B	Zr	Other
Cast alloys																
Alloy 713C	74.0	12.5	0.0	4.2	0.0	0.0	2.0	6.1	0.8	0.0	0.0	0.0	0.12	0.012	0.10	
Alloy 713LC	75.0	12.0	0.0	4.5	0.0	0.0	2.0	5.9	0.6	0.0	0.0	0.0	0.05	0.010	0.10	
CMSX-2	66.0	8.0	4.6	0.6	7.9	5.8	0.0	5.6	0.9	0.0	0.0	0.0	0.00	0.000	0.00	
IN731	67.0	9.5	10.0	2.5	0.0	0.0	0.0	5.5	4.6	0.0	0.0	0.0	0.18	0.015	0.06	1.0V
IN792	61.0	12.4	9.0	1.9	3.8	3.9	0.0	3.1	4.5	0.0	0.0	0.0	0.12	0.020	0.10	
MAR-M 421	61.0	15.8	9.5	2.0	3.8	0.0	2.0	4.3	1.8	0.0	0.0	0.0	0.14	0.015	0.05	
PWA 1480	63.0	10.0	5.0	0.0	4.0	12.0	0.0	5.0	1.5	0.0	0.0	0.0	0.00	0.000	0.00	
Rene 80	60.0	14.0	9.5	4.0	4.0	0.0	0.0	3.0	5.0	0.0	0.0	0.0	0.17	0.015	0.03	
Udimet 500	52.0	18.0	19.0	4.2	0.0	0.0	0.0	3.0	3.0	0.0	0.0	0.0	0.07	0.007	0.05	
IN738LC	63.0	15.7	8.0	1.5	2.4	1.5	0.0	3.2	3.2	0.0	0.0	0.0	0.09	0.007	0.03	0.6 Nb
Wrought alloys																
Astroloy	55.0	15.0	17.0	5.3	0.0	0.0	0.0	4.0	3.5	0.0	0.0	0.0	0.06	0.030	0.00	0.3V
Hastelloy C-22	51.6	21.5	2.5	13.5	4.0	0.0	0.0	0.0	0.0	5.5	1.0	0.1	0.01	0.000	0.00	2.0Cu
Hastelloy G-30	42.7	29.5	2.0	5.5	2.5	0.0	0.8	0.0	0.0	15.0	1.0	1.0	0.03	0.000	0.00	
Inconel 600	76.0	15.5	0.0	0.0	0.0	0.0	0.0	0.0	0.0	8.0	0.5	0.2	0.08	0.000	0.00	
Inconel 718	52.5	19.0	0.0	3.0	0.0	0.0	5.1	0.5	0.9	18.5	0.2	0.2	0.04	0.000	0.00	
Nimonic 80A	76.0	19.5	0.0	0.0	0.0	0.0	0.0	1.4	2.4	0.0	0.3	0.3	0.06	0.003	0.06	
Nimonic 115	60.0	14.3	13.2	0.0	0.0	0.0	0.0	4.9	3.7	0.0	0.0	0.0	0.15	0.160	0.04	
Rene 95	61.0	14.0	8.0	3.5	3.5	0.0	3.5	3.5	2.5	0.0	0.0	0.0	0.15	0.010	0.05	
Udimet 720	55.0	17.9	14.7	3.0	1.3	0.0	0.0	2.5	5.0	0.0	0.0	0.0	0.03	0.033	0.03	
Waspaloy	58.0	19.5	13.5	4.3	0.0	0.0	0.0	1.3	3.0	0.0	0.0	0.0	0.08	0.006	0.00	

The γ' precipitate phase, which can be seen in the binary phase diagram in Figure 1.2, is a long range ordered intermetallic compound with nominal composition of $Ni_3(Al, Ti)$, which forms coherently within the γ matrix phase. γ' precipitates in Ni-base superalloys have been observed firstly as fine spheroidal particles (see Figure 1.3) distributed homogenously, then cuboidal precipitates (see Figure 1.4) have been noticed with higher aluminum and titanium contents [3]. Since Ni-base superalloys derive their high strength from uniform precipitation of γ' phase, volume fraction of γ' is extremely important.

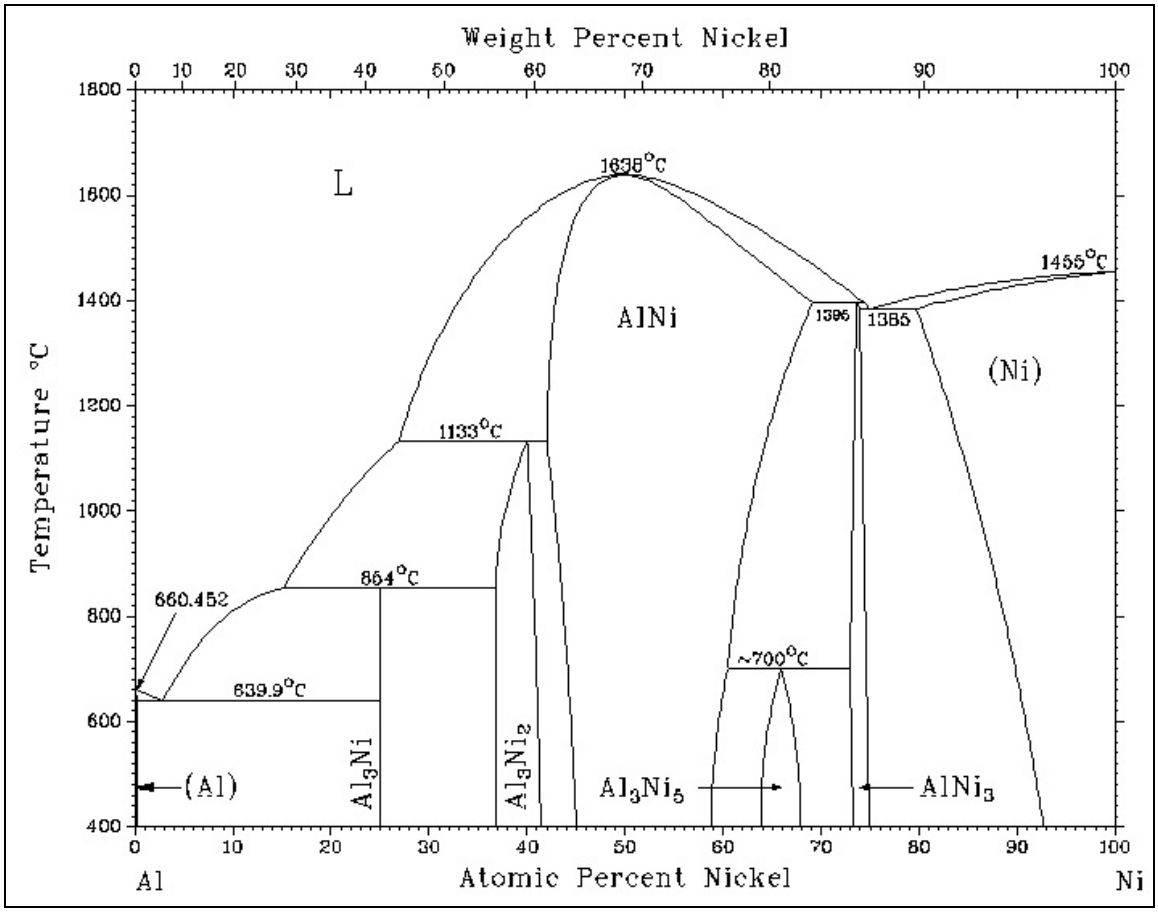

Figure 1.2. Ni-Al binary phase diagram [3]

Carbides are formed with combination of carbon, in amount of about 0.02 to 0.2 weight per cent, and reactive elements, such as titanium, tantalum, hafnium, and niobium. They preferentially form at grain boundaries in Ni-base superalloys, where they prevent grain-boundary sliding, thus improve creep properties. In Figure 1.5, MC and $M_{23}C_6$ type carbides, which are located at grain boundaries, can be seen. As a second task, carbides can

tie up some elements that would promote phase instabilities. MC type carbides may transform into $M_{23}C_6$ and M_6C type carbides under service conditions.

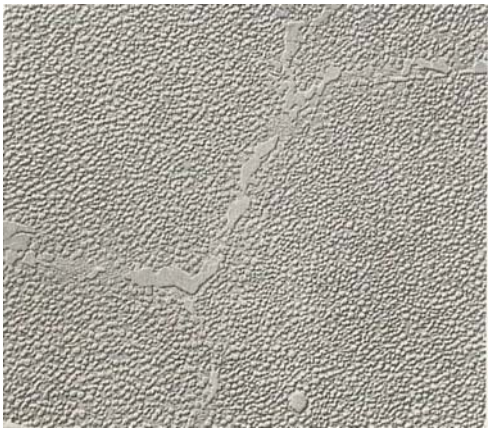

Figure 1.3. Uniformly distributed fine precipitates in AF-1753, mag. 4100x [1]

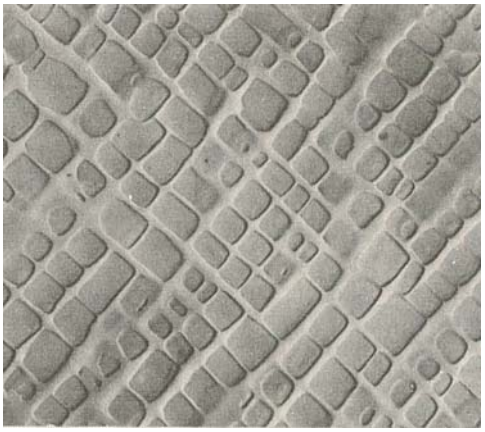

Figure 1.4. Uniformly distributed cuboidal precipitates in IN 100, mag. 13625x [1]

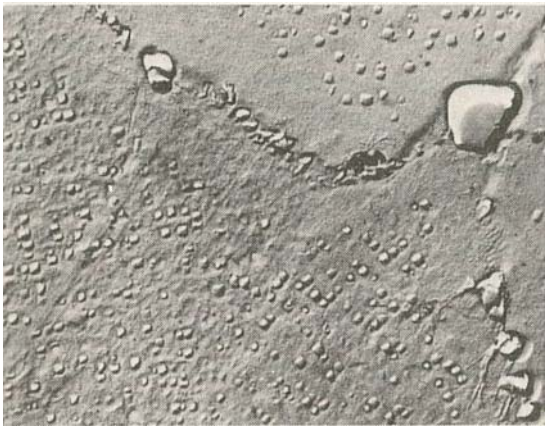

Figure 1.5. Fine $M_{23}C_6$ and coarse MC grain boundary carbides in X-750, mag. 4900x [1]

When the composition of a specific alloy has not been carefully controlled, formation of undesirable phases during service is possible. These phases, which appear generally as plates and needles, have harmful effects on the properties of the alloy. High amounts of body-centered cubic (BCC) transition elements, such as tantalum, niobium, chromium, tungsten, and molybdenum, are mostly responsible for TCP phase formation [3]. σ, μ, and Laves phases are the most known TCP phases which form in Ni-base superalloys.

1.2.2. Strengthening of Nickel-Base Superalloys

The strength of nickel-base superalloys is provided through several hardening mechanisms, such as contribution of solid solution elements, precipitation of intermetallics and carbides, thermomechanical processes to control grain size, and dispersion of oxide particles. It is crucial to note that the most remarkable strengthening effect is obtained by precipitation of intermetallics. Thus, strengthening by precipitation and precipitation mechanisms are the most attractive research topics.

The FCC nickel matrix provides high solubility for many alloying elements because of its electronic structure (nearly filled 3d electron shell). Solid solution strengthening is chiefly formed by lattice distortions. Alloying elements, such as molybdenum and tungsten, are effectively used because of their strong lattice cohesion and diffusion reducing effect. Matrix can also be strengthened via atomic clustering or short range order which is an electronic effect and observed with alloying elements, such as molybdenum and tungsten, together with chromium and aluminum [4]. However, strengthening via short range order rapidly decreases over about 0.6 T_m, where T_m is the melting temperature.

The most effective way to strengthen the matrix of a superalloy is precipitation hardening mechanism, where strength is related to volume fraction, size, morphology, and distribution of precipitates. These second phase particles are generally in the type of γ' [Ni_3(Al, Ti)] or γ'' [Ni_3Nb]. The major factors which play a role in the strengthening of superalloys by precipitation are the coherency strain and the presence of order in the particles. Coherency strains are caused by misfit (lattice size difference) between matrix and precipitate lattices, where misfit, δ is defined by the formula given below [12], in

which d_γ and $d_{\gamma'}$ are the unstressed interplanar spacings of matrix and precipitate phases, respectively.

$$\delta = \frac{d_\gamma - d_{\gamma'}}{d_{\gamma'}} \tag{1.1}$$

Low lattice mismatch ($0 < \delta < 0.01$) between matrix and precipitates is essential for effective strengthening. Also, at least 30 per cent volume fraction of second phase particles is required. Moreover, the precipitates should be stronger than the matrix phase in order to prevent slip cutting [11]. All these factors contribute to strengthening of a superalloy. Thus, microstructural aspects of the alloy should be controlled precisely and precipitate evolution mechanism should be well understood.

1.2.3. Precipitate Evolution Mechanism

Precipitate evolution follows the stages, namely, nucleation, growth, coarsening, and dissolution. Nucleation is the process of formation of a very fine precipitate particle which is called nucleus. Once a nucleus is formed, it starts to grow, by absorbing solute atoms from the solid solution matrix phase. During growth, precipitate volume fraction increases as solute is rejected by the matrix. Precipitates may grow further without any increase in volume fraction, and this stage is called coarsening or Ostwald ripening. Ostwald ripening phenomenon was formulated by Lifshitz and Slyozov [13], and by Wagner [14] separately, but these two works were combined in LSW theory. Several other coarsening theories were suggested based on LSW theory [15-21]. Subsequent to reaching a critical size, precipitates start dissolving back into the matrix. Then, a full circle of all these stages may be defined as the life cycle of a precipitate, where nucleation maybe termed birth and dissolution maybe termed death. In the following sections theoretical and experimental aspects of these stages will be presented as already laid out in the literature.

1.2.3.1. Nucleation. Nucleation may take place homogeneously or heterogeneously. During homogeneous nucleation, γ' forming atoms diffuse into nucleation sites in γ matrix to form a nucleus, and subsequent to solid – solid transformation an interface must be

created which is accompanied by an activation energy barrier [12]. Total free energy change associated with homogeneous nucleation is given by the following equation.

$$\Delta G_{hom} = -V\Delta G_v + A\Gamma + V\Delta G_s \tag{1.2}$$

In this equation, first right hand-side term is related with the free energy reduction caused by the formation of a volume V of γ'. Second term symbolizes a free energy increase which is given by creation of an interfacial area A of γ/γ' interface, where Γ is the interfacial energy. The mismatch between the two phases gives rise to misfit strain energy $V\Delta G_s$. If we assume that precipitates are in the shape of spheroids, than Equation 1.2 will turn into below form where r is the radius of the spheroid.

$$\Delta G = -\frac{4}{3}\pi r^3\left(\Delta G_v - \Delta G_s\right) + 4\pi r^2\Gamma \tag{1.3}$$

In most cases, nucleation in solids is not homogeneous. Dislocations, grain boundaries, stacking faults, and vacancies are adequate nucleation sites. If a nucleus is formed in one of these sites, total free energy decreases because of elimination of a defect which also reduces activation energy barrier [12]. Free energy change associated with heterogeneous nucleation is given below where ΔG_d is released free energy because of eliminated defect.

$$\Delta G_{het} = -V\left(\Delta G_v - \Delta G_s\right) + A\Gamma - \Delta G_d \tag{1.4}$$

The first step in precipitation heat treatments is solutionizing, where existing precipitates and other phases are completely dissolved into matrix, leading to a single phase, super saturated solid-solution. The most attracting topic about nucleation process is cooling precipitates phenomenon which means precipitate formation during cooling subsequent to a solutionizing treatment. This type of heat treatment is sufficient to dissolve all precipitates but as the temperature goes down precipitates start to nucleate again. A number of researchers studied cooling precipitate formation. Henderson and Mclean [22] stated that a 1200°C solution treatment of superalloy IN738LC for 2 hours was sufficient to dissolve all γ' precipitates, but they reformed during accelerated air cooling as a

uniformly fine dispersion. Balikci et al. [23] studied influence of various heat treatments on the microstructure of superalloy IN738LC. They reported that solution treatments at 1120°C and 1200°C for 4 hours followed by water quenching were not proper to obtain a single phase supersaturated microstructure. Moreover, they stated that solution treatments for 24 hours at same temperatures were giving similar results as the previous ones. After a set of treatments, they consequently declared that solution treatments at 1235°C and 1250°C resulted in complete dissolution of γ' precipitates. Safari and Nategh [24] researched heat treatment effects on the microstructure of superalloy Rene 80 and they concluded that solution treatment at 1150°C for 2 hours was not able to dissolve all γ' precipitates.

1.2.3.2. Growth of Precipitates. Subsequent to formation of a nucleus with the smallest critical volume, the γ' precipitate starts to grow. During growth process strain energy effects and interfacial energy minimization principle dictate the shape of the precipitates [12]. Ricks et al. [25] studied the growth and morphological development of γ' particles and they stated that elastic modulus anisotropy in the material causes cuboidal γ' morphology to appear in the early stages of growth. They also reported that γ' particles in nickel-base superalloys follow the morphological development sequence, such as spheres → cuboids → cuboidal arrays → dendrites. A similar sequence is also reported by Grosdidier et al. [26] in a study.

As precipitates may grow with a size distribution which can be conveniently averaged into a single representative size, however in a certain temperature range, a duplex size precipitate microstructure is observed. In a duplex size distribution, a microstructure displays two distinctly different precipitate sizes. Precipitate growth process happens in two different ways; one is through merging of adjacent particles and the other is through solute absorption from the matrix. Balikci et al. [23] observed these two mechanisms. They reported that growth process during any aging treatment subsequent to 1120°C/2h solution treatment was occurring through merging of smaller precipitates into larger ones. Roy et al. [27] studied the precipitate growth features in the duplex size precipitate distribution. They concluded that small precipitates grow faster at high temperatures, finally a single size system forms. They also observed the Precipitate Agglomeration Mechanism (PAM), merging of fine precipitates with each other and with coarse ones.

Roy et al. [27] also studied the growth activation energy requirements and they found out that coarse particles need less activation energy than fine ones. They used LSW [13, 14] formulation, as given by Equation 1.5, to calculate molar activation energies for the coarsening process of both coarse and fine precipitates.

$$d_t^n - d_0^n = K\,t \tag{1.5}$$

In this formula, d_0 is the initial particle size, d_t is the size after heating for time *t*, and *n* is the growth exponent which is generally assumed to be 3 for superalloys. *K* is the rate constant defined as follows:

$$K = K_0 \exp\left(-\frac{Q}{RT}\right) \tag{1.6}$$

Here, *Q* is the molar activation energy for the growth process, *R* is the universal gas constant and *T* is the absolute temperature. As a result, Roy et al. [27] found out that in the case of duplex size microstructure, the activation energy for growth of particles is not constant.

1.2.3.3. Coarsening and Effects of Elastic Interaction. Several theoretical and experimental studies have been conducted about the coarsening mechanisms [28-45]. The driving force for coarsening is minimization of total free energy which previously believed to be consists of interfacial energy and elastic strain energy. But new results introduced that elastic interaction energy between particles also plays an important role in microstructural development of precipitates. At the early stages of coarsening, interfacial energy drives the microstructural evolution where the process takes place by growth of large particles via solute absorption at the expense of smaller ones [38]. As the particles reach a critical size, elastic strain energy and elastic interaction energy start to dominate the process.

Consideration of elastic interaction has started with the celebrated study of Eshelby [46], in which he determined the elastic field around an ellipsoidal inclusion. Following this paper, more theoretical studies have been conducted about elastic interaction energy

and theory has developed step by step [47-63]. It is also utilized to explain some experimental observations such as splitting of precipitates. Miyazaki et al. [55] explained morphological changes during coarsening under external stress by using energy calculations. In another study [58] splitting phenomenon is discussed in an energetic point of view. Elastic interaction energy is taken into account in all of these cited studies.

1.3. Objectives and Scope

Microstructure control is very important for effective use of the nickel-based superalloy IN738LC at high temperatures. Understanding the fundamentals of microstructural evolution is the primary objective of this study. It is well known that material properties are closely related with the material structure and structure is closely related with the processing conditions. In this study, effects of processing conditions on the microstructure are analyzed, but no analysis is conducted to build a relationship between the structure and material properties. This thesis is focused on the evolution mechanism of γ' precipitates.

The work presented in this thesis provides basic data on the complete dissolution of γ' precipitates, their growth characteristics and coarsening behavior. Some heat treatments are conducted to develop different microstructures and results are discussed in a systematic way. The current research aims at completing the missing parts of previous studies conducted about the precipitation mechanisms in the superalloy IN738LC.

2. EXPERIMENTAL PROCEDURE

2.1. Material

This study involves the precipitate evolution in IN738LC, which is a polycrystalline, investment cast, nickel base superalloy. The material was provided by Howmet Corporation, Whitehall, MI, USA, in the form of rods with 15 mm in diameter and 110 mm in length. The as-received material was HIPed (hot isostatically pressed) at 1185°C for 2 hours under a neutral environment in order to remove microporosities. Subsequent to cooling to room temperature, a solution treatment at 1120°C for two hours was conducted. Then, material was aged at 843°C for 24 hours. Both treatments were ended with argon-backfill cooling. The chemical composition of the as-received material is given in Table 2.1, and its precipitated microstructure is shown in Figure 2.1.

Table 2.1. Chemical composition of the as-received IN738LC

Element	Ni	Cr	Co	Mo	W	Ta	Nb	Al	Ti	B	Zr	C
wt.%	balance	15,7 - 16,3	8,0 - 9,0	1,5 - 2,0	2,4 - 2,8	1,5 - 2,0	0,6 - 1,1	3,2 - 3,7	3,2 - 3,7	0,007 - 0,012	0,03 - 0,08	0,09 - 0,13

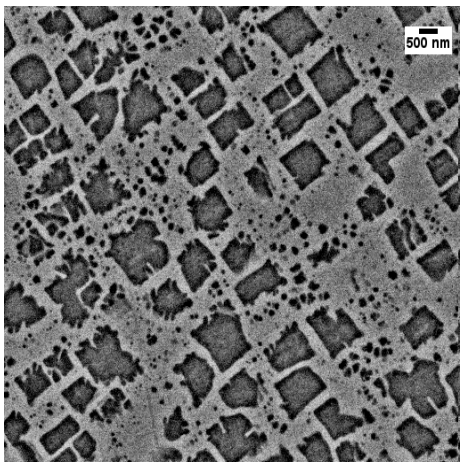

Figure 2.1. Precipitate microstructure of the as-received IN738LC

2.2. Heat Treatments

Several samples of IN738LC were prepared for various heat treatments. They were cut from as-received cylindrical bars by using a Struers-Minitom diamond blade, precision cutting machine, which was operated at speeds in the range 250-300 rpm with proper coolant. Then, they were cleaned in an ultrasonic cleaner and wrapped with a stainless steel foil in order to prevent any interaction between the samples and their quartz container. Wrapped samples were sealed in quartz tubes under vacuum by using oxy-acetylene flame torch. Before the sealing, the quartz tubes were first evacuated and then purged with 99.999% purity argon three times. A mechanical pump was used to provide 10^{-4} mbar vacuum. Subsequent to sealing, quartz tubes were put on an alumina piece and placed in a horizontal tubular furnace which is in fact tiltable upto 90°. Schematic representation of the furnace is given in Figure 2.2. Alumina was required to prevent any reaction between quartz tube and surface of the furnace mullite tube. The temperature at the sample location was measured with an R-type thermocouple. At the end of heat treatments, samples were quickly quenched in the water (WQ) by tilting the furnace or they were cooled in furnace (FC) by power shutdown. Heat treatment schedules are given in Table 2.2 and described in the following sections.

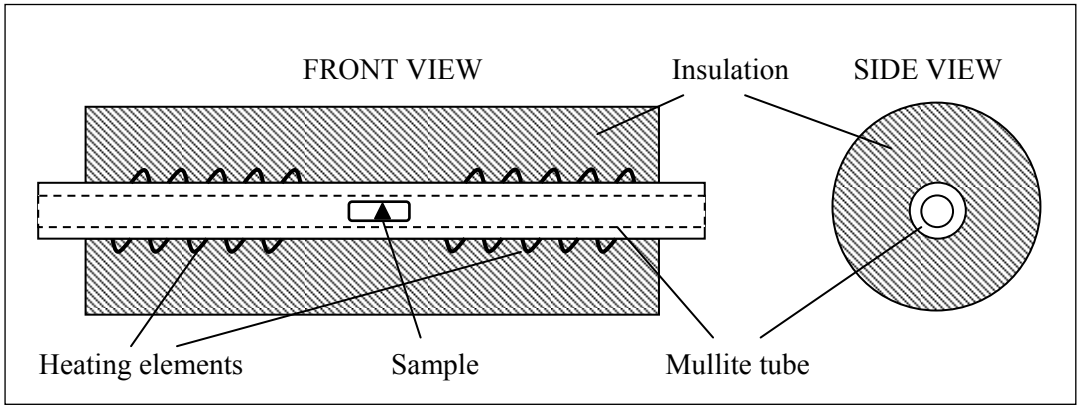

Figure 2.2. Schematic of the tubular furnace

2.2.1. Treatments for Analysis of Cooling Precipitates

The samples were heated at 1235, 1250 and 1300°C for 4 hours and then quenched in water. This procedure, a solutionizing heat treatment, was carried out to find out if

precipitates formed or not; that is to see if a fully supersaturated solid solution was obtained.

2.2.2. Treatments for Analysis of Shape and Size Evolution

Two different sets of shape/size evolution treatments were carried out. In the first, a solution treatment to the samples was given (1200°C/4h/WQ) which produced a fine size (50 nm) precipitate microstructure. Then, samples were aged at 1140°C for 1, 5, 10, 15, 20, 30 minutes. A previous study revealed that a duplex-size precipitate microstructure appeared after an aging for 30 minutes [7]. However, it wasn't made clear whether this type of microstructure formed right at the 30^{th} minute or any time earlier. Current study was conducted to determine the exact formation time of duplex-size microstructure and also explore the mechanism for growth/shape change from spheroidal to cuboidal. Aging at this high temperature (1140°C) was preferred since this would accelerate the growth process.

In the second, coarsening was investigated subsequent to dissolution of coarse precipitates. Once precipitates reached a critical size in unimodal cuboidal form, they started shrinking in size after agings upto 24 hours at 1120°C. This study was also aimed at discovering the extent of this reduction in size. For this, the samples were first given a solution treatment (1200°C/4h/WQ); afterwards, they were all aged at 1120°C/24h/FC to grow in size up to 1000 nm, which was defined as the critical size, after which dissolution mode sets in. Cooling characteristic of the furnace is given in Figure 2.3. Subsequent agings longer than 24 hours caused further coarsening of the particles. It was aimed at observing different forms of coarsening. Subsequent to the first aging treatment, these samples were aged for longer times (12, 72, 144, 216, 288 hours) still at 1120°C, during which dissolution/growth was expected.

2.2.3. Treatments for Analyzing Effects of Actual Thermal Conditions

The superalloy IN738LC is generally utilized between 800-1000°C. Some samples have been aged at 950°C for various times (1, 3, 6, 12, 24, 48, 96, 240, 480 hours) to find out the evolution of the two distinctly different size of precipitates (duplex size) at a

temperature in this range for elongated time of utilization. The initial precipitate microstructure for this analysis is obtained with a preliminary aging treatment of 1140°C/4h/WQ subsequent to a solution treatment of 1200°C/4h/WQ which gives a duplex-size microstructure, composed of ~50 nm size fine precipitates and ~450 nm size coarse precipitates.

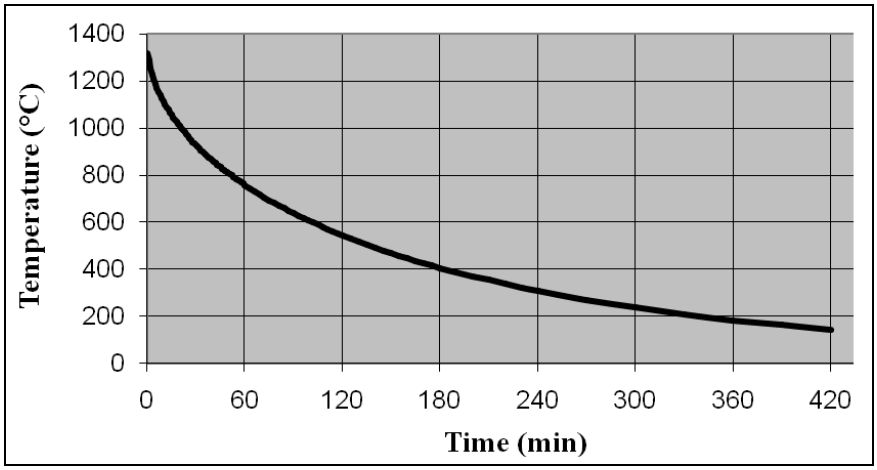

Figure 2.3. Furnace cooling curve that starts from 1300°C

Table 2.2. Heat treatment schedules

Solution Treatment	**Aging Treatment**
T / 4h /WQ T = 1235, 1250, 1300°C	N/A
1200°C/4h/WQ	1140°C/t/WQ t = 1, 5, 10, 15, 20, 30 minutes
1200°C/4h/WQ	1120°C/24h/FC + 1120°C/t/WQ t = 0, 12, 72, 144, 216, 288, 480 hours
1200°C/4h/WQ	1140°C/4h/WQ + 950°C/t/WQ t = 1, 3, 6, 12, 24, 48, 96, 240, 480 hours
WQ = water quenched; FC = furnace cooled; h = hours; t = time	

2.3. Metallography, Electron Microscopy, and Image Analysis

After various heat treatments, samples were broken out of their quartz tubes and prepared for microstructure characterization. For this, the samples were ground using grinding papers with SiC abrasive particles. Several sand papers were used with coarse to fine grit size (120, 240, 320, 400, 600, 800, 1200). Subsequent to grinding, the samples were polished on rotating wheels with fine alumina powder of size 1, 0.3, 0.05 micron. Buehler-Phoenix Beta grinding-polishing unit was employed for these operations. After cleaning in an ultrasonic bath, they were etched with a solution of composition (in volumes) 33% HNO_3 + 33% acetic acid + 33% H_2O + 1% HF. A Philips XL30 ESEM-FEG/EDAX system was used to characterize the distribution and morphology of γ' precipitates. Backscattered electron (BSE) mode was used in SEM because of its higher energy and composition sensitivity. Micrographs were recorded at 15000x, 30000x, 50000x and 100000x (if required) magnifications.

Size and area fraction of the γ' precipitates in various conditions were measured from the digital micrographs, directly acquired from the SEM, using an image analysis software. Reported precipitate sizes were obtained after measuring as many particles as possible in the representative micrographs. In the case of duplex microstructure, coarse and fine precipitates were measured separately.

3. RESULTS & DISCUSSIONS

3.1. Microstructure Characterization

Chemical composition of the precipitates in the IN738LC was analyzed in an earlier study [23] and analysis showed that they were of the intermetallic $Ni_3(Al, Ti)$, γ' phase with the $L1_2$ ordered FCC superlattice structure. In the current study, the volume fraction of the γ' precipitates was determined to be 42% in the FC (furnace cooling after aging) condition which is consistent with the data given in the literature [23, 27, 66].

3.2. The Cooling Precipitates Phenomenon: Solution Treatments above 1200°C

Commercial heat treatments for superalloys generally consist of two steps; solutionizing and aging. In this part of the thesis, results of the solution treatments carried out at different temperatures are presented and discussed. Solution treatments were conducted at 1235, 1250, and 1300°C for 4 hours each and all specimens were subsequently water quenched. In a previous study [23], it was stated that solution treatments of IN738LC at 1120 and 1200°C were not sufficient to dissolve all γ' precipitates. It was also reported that solution treatments at 1200°C, which was selected as the solutionizing temperature in most of the heat treatment procedures of this study, produced a very fine precipitate microstructure (~50 nm precipitate size). In order to determine the exact temperature range for complete dissolution, three solution treatments were carried out at temperatures mentioned above. For all three cases, complete dissolution of γ' phase was obtained. When these results are combined with the ones given in the literature, it is obvious that any temperature below 1235°C is not sufficient to dissolve all the precipitates. On the other hand, it can be concluded that solutionizing temperatures below 1235°C may be employed for precipitate particle refinement [23]. It should be noted that, microstructural characterizations were conducted with a field emission gun – scanning electron microscope (FEG-SEM) with 2 nm resolution, thus all these results are obtained in the limits of FEG-SEM.

Another important discussion regarding the dissolution of precipitates is the reformation of particles during quenching, which are generally called cooling precipitates. It is believed that after a complete dissolution of second phase particles, they can reform by a spinodal type transformation even with high cooling rates. Spinodal decomposition is a diffusional phase transformation where there is no nucleation barrier. Thus, this type of transformations cannot be impeded. Some authors [22, 23] discussed formation mechanism of fine precipitates. Henderson and McLean [22] reported that solution treatment at 1200°C was sufficient to dissolve precipitates completely, but they reformed during cooling. Contrary, current study confirmed that 1200°C was not sufficient to dissolve all the γ' precipitates, but any solutionizing treatment above 1235°C resulted in a single phase solid solution. Therefore, it can be concluded that fine precipitate formation is not a spinodal type transformation. A possible explanation for previous observations may be insufficient thermal energy for complete dissolution. As proposed above, any solutionizing temperature below 1235°C can be employed for particle refinement.

3.3. The Formation of Duplex Microstructure: Agings at 1140°C Subsequent to Solution Treatment at 1200°C/4h/WQ

As reported by Balikci et al. [67, 68], aging treatments at 1140°C produce a duplex precipitate size microstructure. In the current study, aging treatments at 1140°C for 1-30 minutes were carried out subsequent to solutionizing at 1200°C for 4 hours. Aim of these heat treatments was determination of the exact formation time of a duplex-size microstructure which consists of both fine and relatively coarse γ' precipitates. Previously, it was reported that duplex-size microstructure could be observed after an aging treatment for 30 minutes [67, 68]. But no aging heat treatment was conducted between 5 and 30 minutes. Thus, it was not clear that duplex-size microstructure was obtained right at 30^{th} minute or before. In this study, aging treatments were conducted for 1, 5, 10, 15, 20 and 30 minutes and micrographs are given in Figure 3.1a-f, where dark grey regions are the precipitates and light grey region is the matrix. It was observed that after agings for 10 minutes very fine precipitates became visible as can be seen in Figure 3.1c. After 15 minutes, duplex-size microstructure could be seen clearly (Figure 3.1d).

1200°C/4h/WQ solution treatment gave a well-dispersed, very fine microstructure with ~50 nm sized spheroidal precipitates, but the aging treatments at 1140°C resulted in a duplex-size microstructure, as stated above. Formation of this microstructure was happened via growth of some of the fine precipitates through solute absorption from the matrix, while other particles maintained their situation. In fact, most probably the growth of some precipitates started in the first minute of the aging, but a distinct duplex-size became visible after 10 minutes. The current observations were done with field emission gun SEM with a higher resolution than the previously used [13, 14] tungsten filament gun SEM. Hence, the observation of the duplex size at a shorter aging time may be attributed to the higher resolution used in this current work. Perhaps, a TEM (Transmission Electron Microscope) may clearly demonstrate the exact time for the formation of the duplex microstructure. It was also observed that precipitates changed their spheroidal morphology to cuboidal form in 10 minutes. This finding can be explained in an energetic point of view (see Equation 1.2). It is known that at small particle sizes, surface energy is dominant; therefore particles assume the spheroidal morphology to lower their surface area. As size increases, volume energy and elastic strain energy starts to dominate the system and it can be resulted in different morphologies (cuboidal in this case) due to anisotropy in elastic properties.

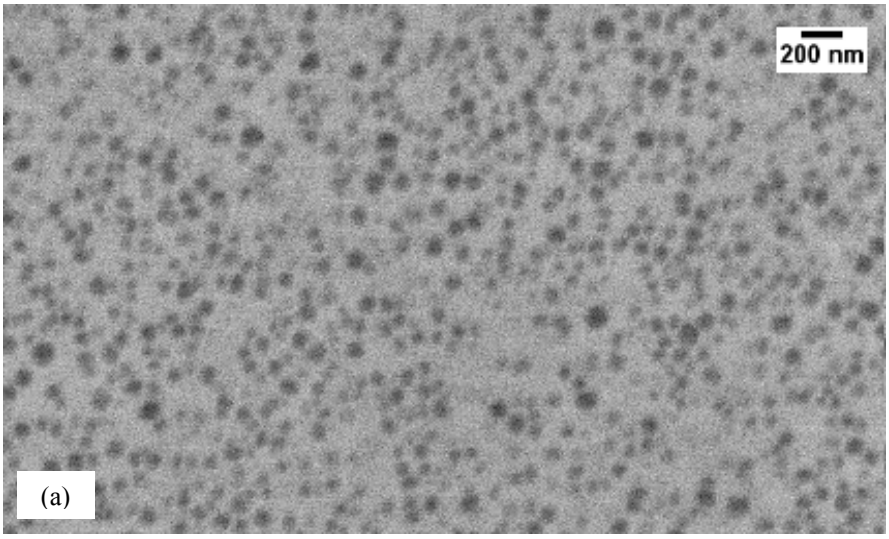

Figure 3.1. Microstructures obtained after 1140°C/t/WQ aging treatments subsequent to 1200°C/4h/WQ solution treatment, (a) t = 1 min, (b) t = 5 min, (c) t = 10 min, (d) t = 15 min, (e) t = 20 min, (f) t = 30 min

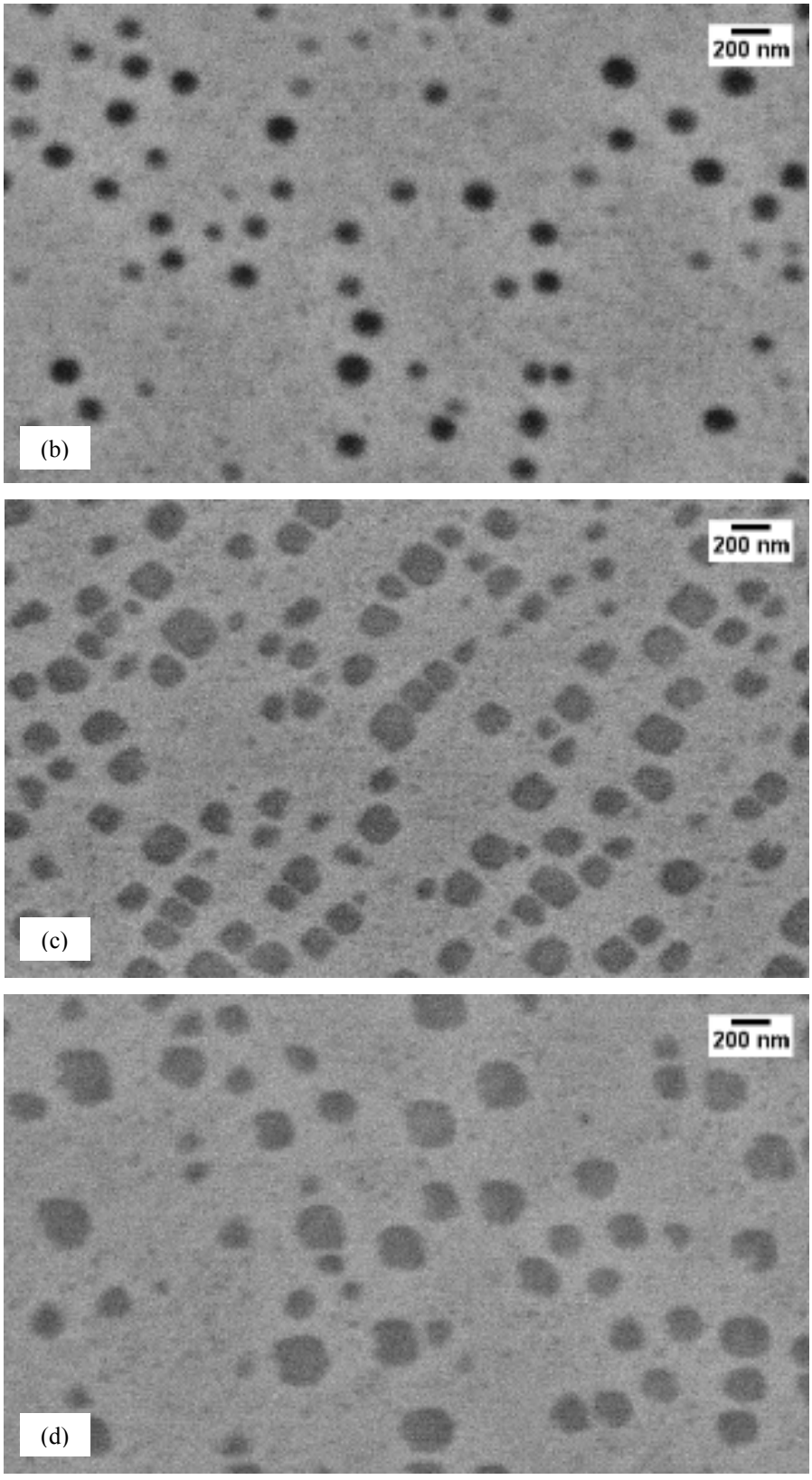

Figure 3.1. Microstructures obtained after 1140°C/t/WQ aging treatments subsequent to 1200°C/4h/WQ solution treatment, (a) t = 1 min, (b) t = 5 min, (c) t = 10 min, (d) t = 15 min, (e) t = 20 min, (f) t = 30 min, *continued*…

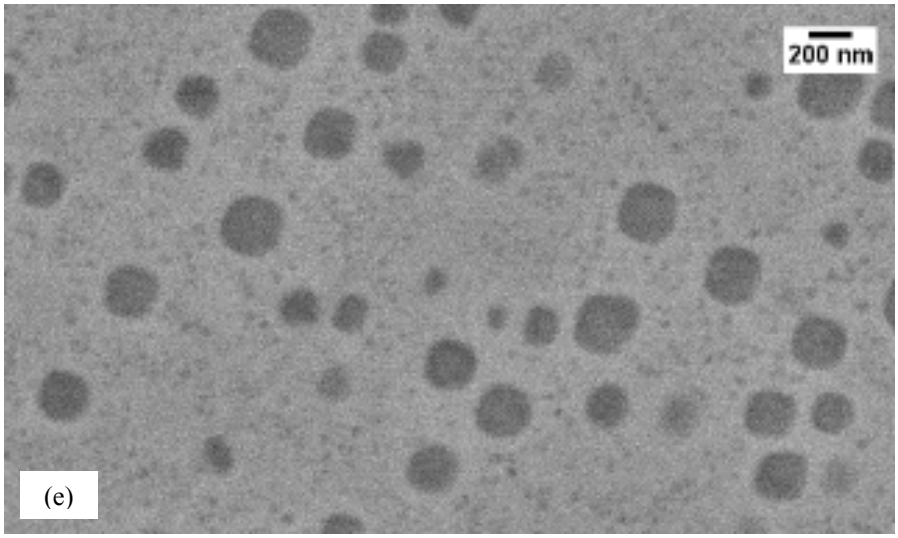

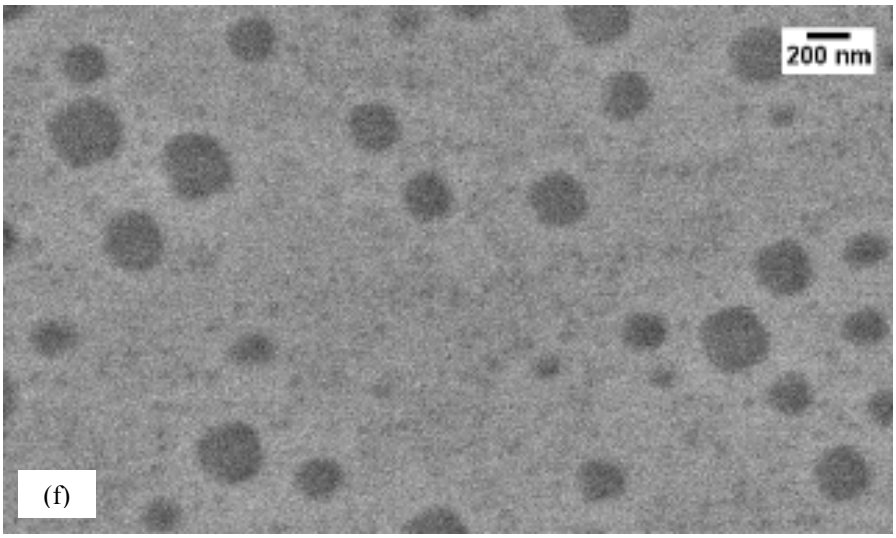

Figure 3.1. Microstructures obtained after 1140°C/t/WQ aging treatments subsequent to 1200°C/4h/WQ solution treatment, (a) t = 1 min, (b) t = 5 min, (c) t = 10 min, (d) t = 15 min, (e) t = 20 min, (f) t = 30 min, *continued*...

A previous study [68] reported longer times of aging at this temperature and authors stated that precipitates continued their growth in cubic morphology upto 24 hours. Then, particles started to change into spheroidal shape by the addition of adjacent precipitates onto flat surfaces of cuboidal precipitates and by the dissolution of corners. This process resulted in initial bulging of the cuboidal precipitates which led the way to mostly spheroidal or irregularly shaped larger precipitates. It is plausible to state that the microstructure tries to reduce the total internal energy by minimizing the surface area. The authors also reported that aging treatments at 1150°C gave a similar duplex-size

microstructure, but any treatments above 1150°C resulted in a single-size microstructure. Therefore, it can be concluded that 1150°C is a critical aging temperature and any temperature between 1150 and 1235°C can be used for particle refinement purposes.

Precipitate size analysis was conducted for all the specimens and results are given in Table 3.1 and plotted in Figure 3.2. The data are for coarse precipitates; fine precipitates do not show any measurable size variation after 1140°C/t/WQ agings. Vertical lines at each point show the maximum and minimum size data obtained for the particular heat treatment. It was reported that precipitates grew to the size of 450 nm in 24 hours [68]. It is clear that growth rate is decreasing with increasing aging time; precipitates gained almost 200 nm in 30 minutes and only 200 nm more in the next 23.5 hours.

Table 3.1. Particle size analysis results for 1200°C/4h/WQ + 1140°C/t/WQ

Aging time (minutes)	Mean size (nm)	Number of particles	Min. size (nm)	Max. size (nm)	Standard deviation
5	129	47	99.36	185.40	23.46
10	173	60	99.36	292.39	45.52
15	209	44	99.36	311.23	58.08
20	238	33	113.18	344.41	61.78
30	251	22	99.36	367.99	74.09

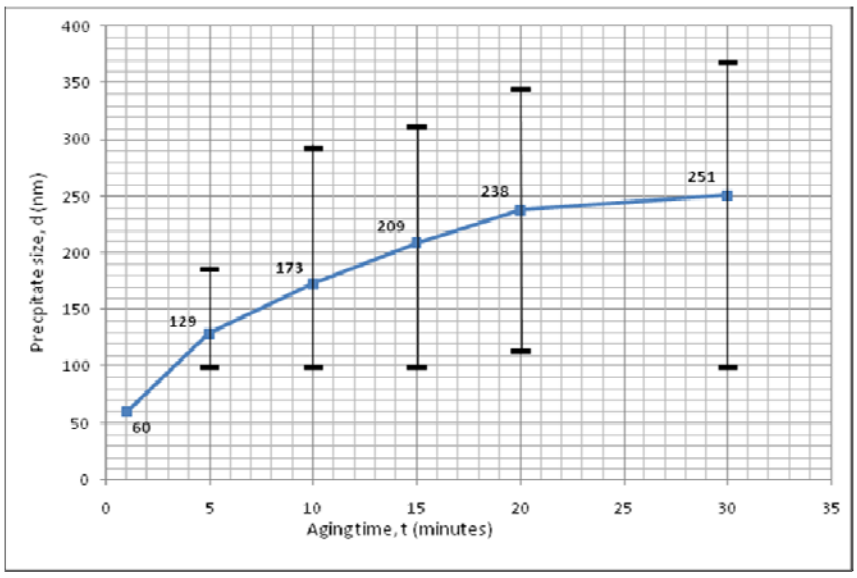

Figure 3.2. Precipitate size variation with aging time at 1140°C. The mean precipitate size at its respective aging time is positioned over the curve.

3.4. The Precipitate Dissolution and Coarsening: Aging Treatments at 1120°C Subsequent to 1200°C/4h/WQ + 1120°C/24h/FC

In order to study dissolution of coarse precipitates and understand further evolution of these particles, a two-step aging procedure was employed. First aging was conducted at 1120°C for 24 hours and ended with furnace cooling. This step resulted in an almost unimodal cuboidal precipitate microstructure with 42% volume fraction where precipitates were in the size of approximately 1000 nm. This microstructure is seen in Figure 3.3. Subsequently, samples were heat treated at the same temperature for different holding times, such as 12, 72, 144, 216, 288, and 480 hours, then water quenched. Results showed that the precipitate size initially decreased due to the dissolution which occurred up to 12 hours where formation of fine precipitates was already started. Balikci et al. [68] stated that coarse precipitates were dissolved along the cube corners which caused change in morphology from cuboidal to spheroidal. This situation was observed after 5 minutes of aging. In the current study, after 12 hours of aging, precipitates were transformed to spheroidal shape likely by a similar mechanism.

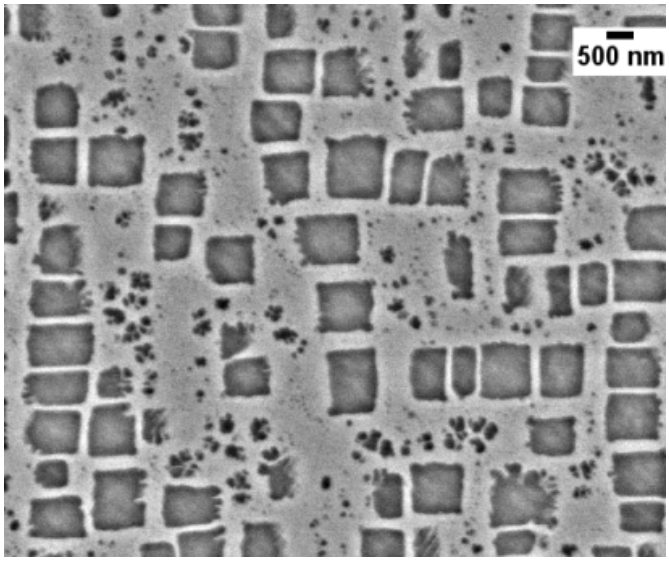

Figure 3.3. Microstructure obtained after 1200°C/4h/WQ + 1120°C/24h/FC

The comparison of the current observations with data reported earlier indicates that precipitate dissolution starts much faster at higher aging temperatures. For example, while dissolution was reported to start after 200 hours at 1100^{o}C [69], it started in 5 minutes at 1140^{o}C and in one second at 1160^{o}C at which temperature 700 nm size cuboidal

precipitates were shrunk into about 70 nm size precipitates, still with a very few large ones [65].

Aging treatments for 72, 144, 216, 288, and 480 hours resulted in particle coarsening that followed initial decrease in size due to dissolution. Size analysis showed that precipitates grew relatively fast up to 144 hours, and then growth rate dropped distinctly. This visible sluggishness probably happened due to a decrease in local solute concentration and also perhaps due to a sharp reduction in total internal energy of the precipitate microstructure. The total energy of such a microstructure has contributions from the interfacial energy and the mismatch energy due to coherency. The precipitates can grow in coherent form with a high coherency energy contribution to the total energy. When the coherency is lost, the contributing factor is only the interfacial energy. Thus, the microstructure may reduce its energy by minimizing the particle surface area.

The data in Table 3.2 and Figure 3.4 suggests that the precipitates cannot grow beyond 1000 nm size in cuboidal form. Hence, they start dissolving which results in a reduction in mismatch (coherency) strain energy. This process transforms the particle morphology to a spheroidal one after which most probably the lattice match is lost. Moreover, the spheroidization of the particles also reduces the interfacial energy contribution to the total energy. The coalescence of these spheroidal particles leads to coarsening and further decrease in the energy.

Table 3.2. Particle size analysis results for 1200°C/4h/WQ + 1120/24h/FC +1120°C/t/WQ

Aging time, t (hours)	Mean size (nm)	Number of particles	Min. size (nm)	Max. size (nm)	Standard deviation
0	1000	111	600	1500	228
12	750	89	200	1200	247
72	950	63	300	1800	333
144	1195	33	600	2200	434
216	1210	48	360	2250	516
288	1220	38	300	1890	520
480	1255	31	565	2160	619

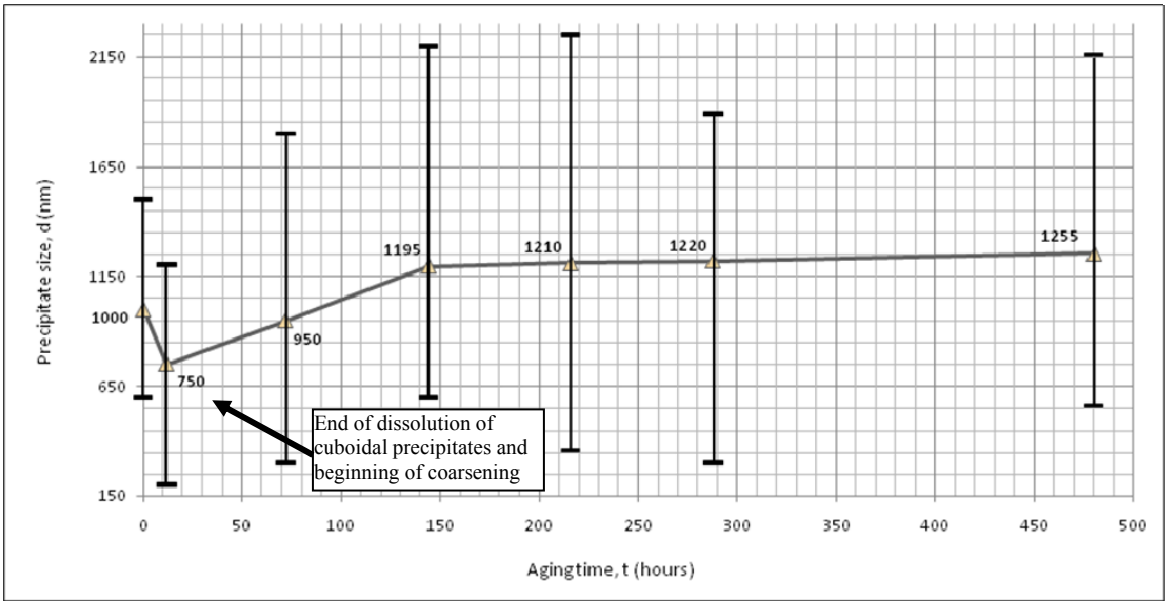

Figure 3.4. Precipitate size variation with aging time at 1120°C. The precipitate size at its respective aging time is positioned over the curve.

Precipitate coarsening is generally explained by Ostwald ripening mechanism. According to this theory, the microstructure of an alloy is always unstable unless the total surface energy is minimized. Thus, larger particles grow at the expense of smaller ones. Ostwald ripening mechanism was observed in the aging treatments reported in this section, but another mechanism was also observed, which is called precipitate agglomeration mechanism (PAM) and it was first proposed by Balikci et al. [23]. This theory suggests that second phase particles move as a whole and coalesce. This type of coarsening was also reported by Prikhodko and Ardell [70]. Agglomeration of equal-sized particles was observed in different samples and some examples are marked in Figures 3.5b, d, e. On the other hand, some of the precipitates were seen lying very close each other, but separated by a thin layer of matrix phase, as shown in Figure 3.5f. This situation can be explained by antiphase boundary (APB) effect. When two independently nucleated domains meet, they can be either in-phase or out-of-phase [12]. If they are out-of-phase, a high energy region would form which is called APB. Therefore, it can be concluded that particles with different domains cannot merge or they need impossibly higher energy to merge.

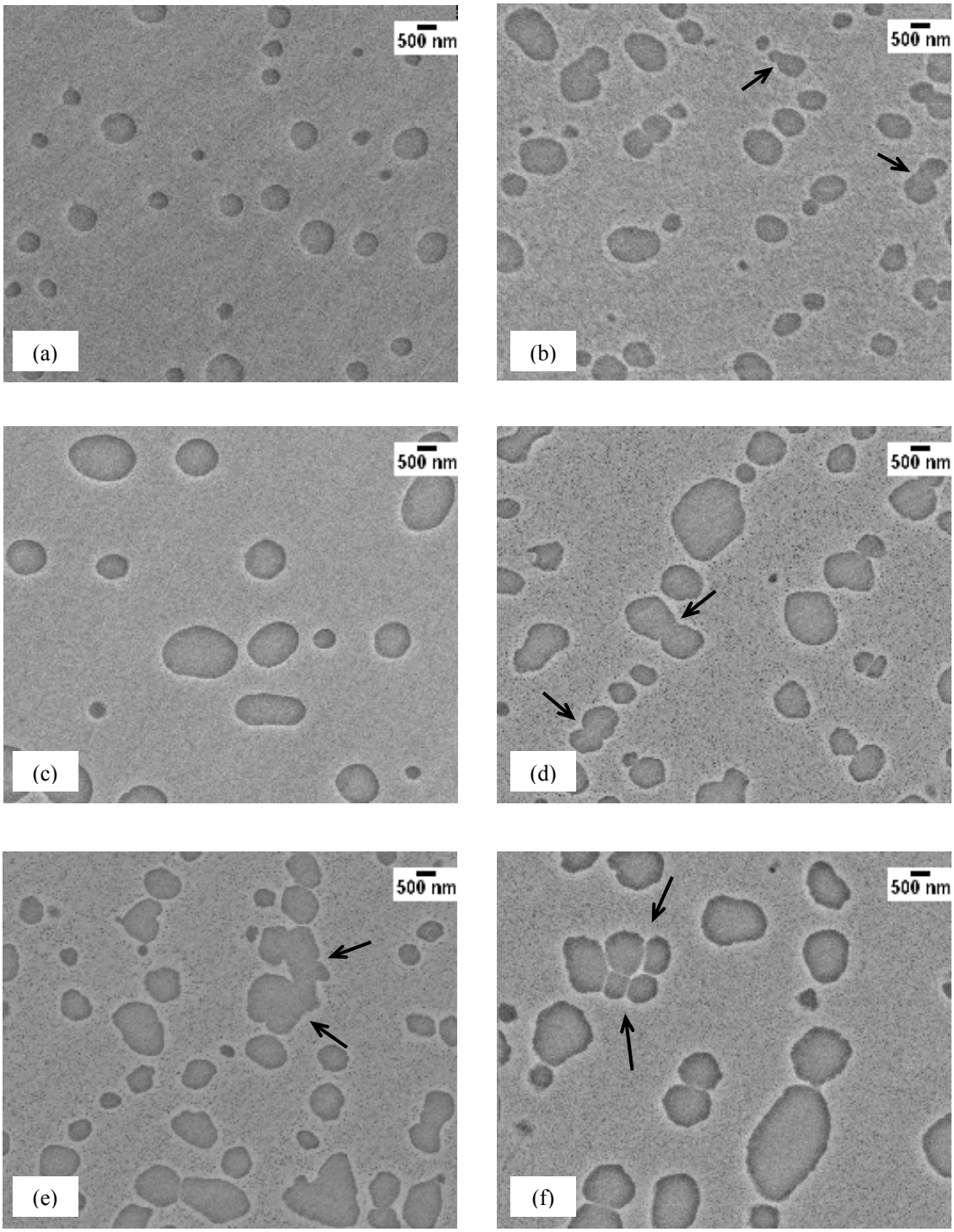

Figure 3.5. Microstructures obtained after 1120°C/t/WQ subsequent to 1200°C/4h/WQ + 1120°C/24h/FC treatments, (a) t = 12 hours, (b) t = 72 hours, (c) t = 144 hours, (d) t = 216 hours, (e) t = 288 hours, (f) t = 480 hours

3.5. The Precipitate Evolution in the Duplex-Size Microstructure: Aging Treatments at 950°C Subsequent to 1200°C/4h/WQ + 1140°C/4h/WQ

The reason for strengthening of materials is impeding the movement of dislocations. Therefore precipitate size, morphology, and distribution is extremely important. The coherency between the precipitate and matrix can also aid strengthening. It's known that uniformly distributed fine precipitates with optimum volume fraction provide the most effective condition to inhibit dislocation motion. Thus, a microstructure which includes fine precipitates should be employed to obtain high strengths at high temperatures. Current study presented in this section of the thesis concerns about the evolution of the microstructure at approximate utilization temperature for the IN738LC.

Superalloys are generally employed at temperatures between 650-1000°C. Balikci et al. [71] studied the tensile properties of IN738LC at 650, 750, and 850°C, and they reported that a duplex-size microstructure (50 nm and 450 nm sized precipitates) showed better mechanical properties. In this present study, aging heat treatments at 950°C were carried out up to 480 hours. Prior to aging heat treatments, samples were solution treated at 1200°C for 4 hours and pre-aged at 1140°C for 4 hours. All heat treatments were ended with water quenching.

Results showed that one hour aging heat treatment showed a duplex-size microstructure, where larger precipitates were in an incomplete cuboidal shape, as seen in Figure 3.6a. The morphology changed into cuboidal after 3 hours of aging. The coarse precipitates retained their cuboidal morphology upto 48 hours then started to become spheroidal by the mechanism of corner dissolution which in fact started after 24 hours as marked in Figure 3.6e and addition of solute atoms to flat surfaces, which was also mentioned in Section 3.4. After the 96-hour aging, all coarse precipitates were transformed into spheroidal morphology, and they continued to grow in spheroidal morphology. While coarse precipitates were growing and changing their morphology from cuboidal to spheroidal, fine precipitates joined together or joined into the coarse ones.

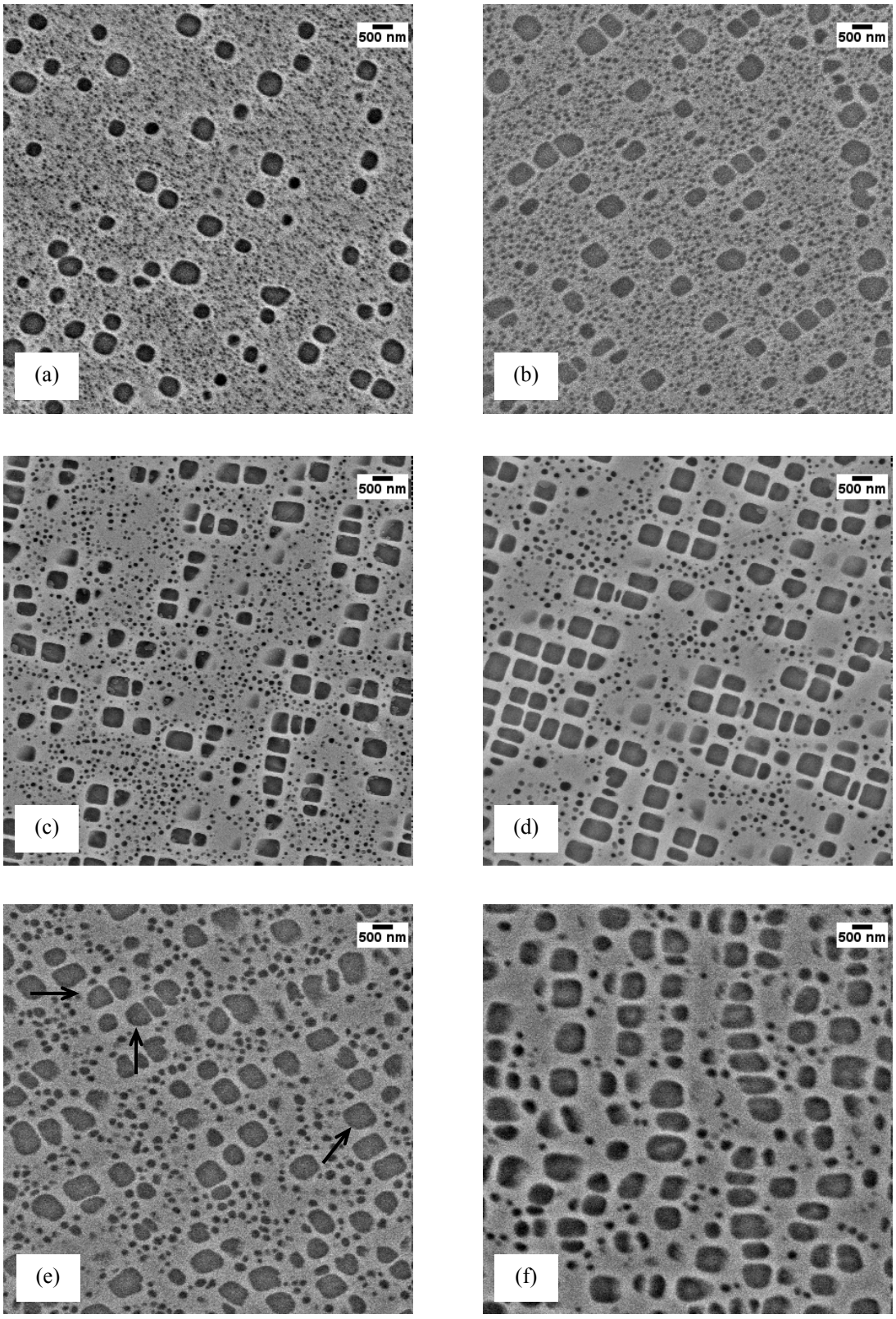

Figure 3.6. Microstructures obtained after 950°C/t/WQ subsequent to 1200°C/4h/WQ + 1140°C/4h/WQ treatments, (a) t = 1 hours, (b) t = 3 hours, (c) t = 6 hours, (d) t = 12 hours, (e) t = 24 hours, (f) t = 48 hours, (g) t = 96 hours, (h) t = 240 hours, (i) t = 480 hours

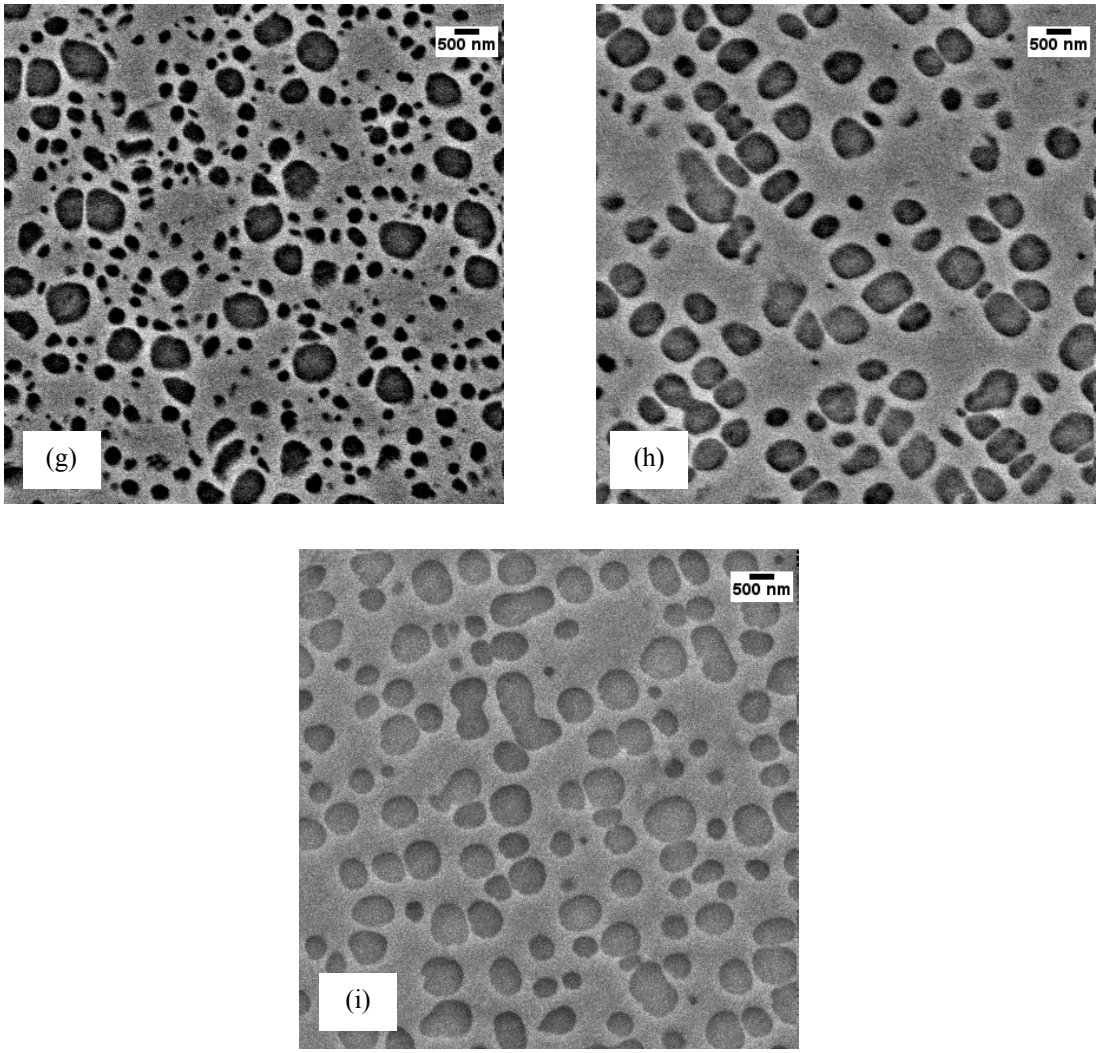

Figure 3.6. Microstructures obtained after 950°C/t/WQ subsequent to 1200°C/4h/WQ + 1140°C/4h/WQ treatments, (a) t = 1 hours, (b) t = 3 hours, (c) t = 6 hours, (d) t = 12 hours, (e) t = 24 hours, (f) t = 48 hours, (g) t = 96 hours, (h) t = 240 hours, (i) t = 480 hours, *continued…*

Size evolution data for coarse and fine precipitates is given in Table 3.3 and Figure 3.7. It's clear that fine precipitates were growing faster than the coarse ones. As a result of this, the size difference between coarse and fine precipitates decreased; size difference of 558 nm at 96 hours compared to 425 nm at 480 hours. Micrographs taken subsequent to each aging step can be seen in Figure 3.6a-i.

Table 3.3. Particle size analysis results for 1200°C/4h/WQ + 1140/4h/WQ +950°C/t/WQ

	Aging time, t (hours)	Mean size (nm)	Number of particles	Min. size (nm)	Max. size (nm)	Standard deviation
Coarse precipitates	1	495	152	200	900	164
	3	500	158	300	1100	166
	6	505	56	300	800	133
	12	510	83	300	800	123
	24	681	158	400	1100	134
	48	692	161	500	1100	116
	96	853	83	600	1200	154
	240	915	142	600	1500	183
	480	955	34	640	1400	219
Fine precipitates	1	55	5455	32	200	32
	3	56	12053	32	300	36
	6	63	975	31	300	46
	12	65	827	31	300	50
	24	206	821	100	400	56
	48	282	313	100	500	106
	96	295	786	32	600	145
	240	435	112	100	600	143
	480	530	19	280	600	96

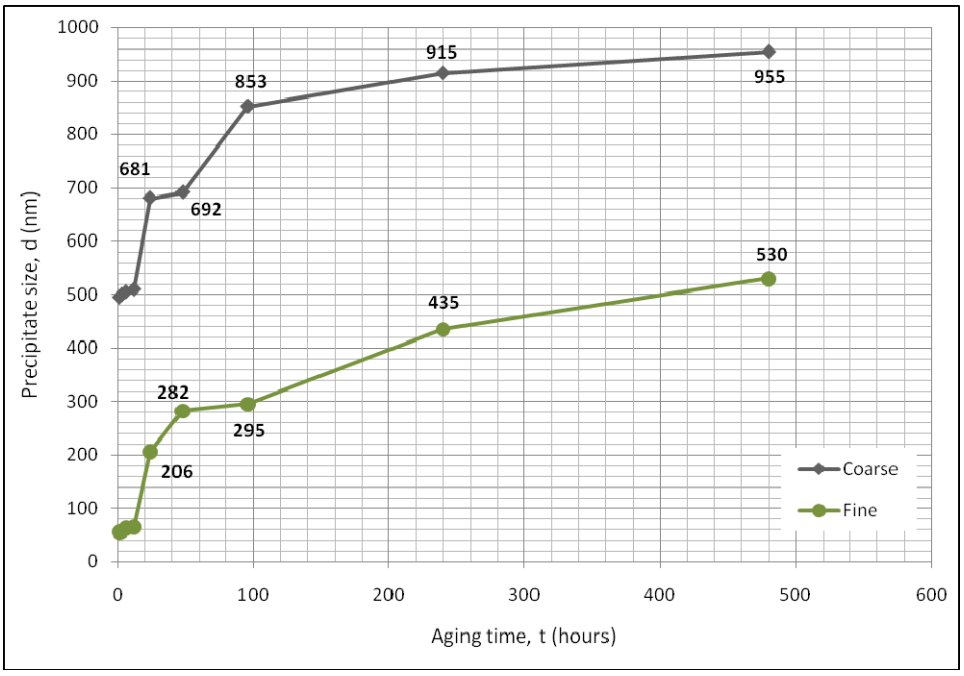

Figure 3.7. Precipitate size variation with aging time at 950°C

In the first steps of the aging, the superalloy maintained its duplex-size microstructure, but it was obvious that IN738LC was not metallurgically stable at 950°C for long times. Both fine and coarse precipitates showed a sharp increase in size in the first 100 hours of aging. Although the growth rate has decreased after 100 hours, but it can be concluded that IN738LC with duplex microstructure is not suitable for applications at and above 950°C because of microstructural instability.

4. CONCLUSIONS

Concluding remarks are listed below:

- Any temperature above 1235°C is sufficient for complete dissolution of γ′ precipitates.
- Cooling precipitate formation is hindered which means that these precipitates do not form via a spinodal type transformation.
- Growth characteristics at 1140°C have been investigated and a duplex-size microstructure has formed after 10 minutes of aging treatment. Furthermore, the precipitate morphology has changed from spheroidal to cuboidal in 10 minutes.
- A number of heat treatments have been conducted at 1120°C to study dissolution and coarsening features of γ′ precipitates. Results have showed that dissolution has occurred upto 12 hours of aging and morphology have changed from cuboidal to spheroidal. Longer aging heat treatments at this temperature have resulted in coarsening of particles.
- Precipitate coarsening has been observed to happen via two different mechanisms; Ostwald ripening and precipitate agglomeration mechanism (PAM).
- The anti-phase boundary (APB) effect has prevented agglomeration of precipitates.
- Some aging heat treatments have been conducted at approximate utilization temperature (950°C) of IN738LC. Results have showed that fine precipitates have grown faster than the coarse ones, but the maximum aging time in this study (480 hours) is not sufficient to obtain a single-size microstructure.
- It has been also shown that a duplex-size microstructure is not metallurgically stable at 950°C, which means that IN738LC is not a suitable material for uses at this temperature.

5. FUTURE WORK

Some suggestions for future work are listed below:

- TEM (transmission electron microscopy) analysis can be conducted to reveal very fine precipitates (if they exist) in the solution treated samples.
- Further size data can be obtained at different temperatures with same aging times to calculate activation energies for fine and coarse precipitates in the duplex-size precipitate microstructures. Activation energies would help to evaluate coarsening behavior of precipitates.
- Micro-hardness tests can be conducted to assess mechanical properties with different microstructures.
- A mathematical model can be employed to determine energy differences before and after particle agglomeration. Since microstructural changes can only happen in a way that minimizes the energy, these calculations would make it clear if precipitate agglomeration is energetically favorable or not.

REFERENCES

1. Sims, C.T. and W.C. Hagel (editors), *The Superalloys*, John Wiley & Sons, USA, 1972.

2. Sims, C.T., N.S. Stoloff and W.C. Hagel (editors), *Superalloys II*, John Wiley & Sons, USA, 1987.

3. Davies, J.R. (editor), *ASM Specialty Handbook – Heat Resistant Materials*, ASM International, 1999.

4. Durand-Charre, M., *The Microstructure of Superalloys*, Gordon and Breach Science Publishers, 1997.

5. McLean, M., "Nickel-base Superalloys: Current Status and Potential", *Phil. Trans. R. Soc. Lond. A*, Vol. 351, pp. 419-433, June 1995.

6. Sims, C.T., "A Contemporary View of Nickel-Base Superalloys", *Journal of Metals*, Vol. 18, No. 10, pp. 1119-1130, October 1966.

7. Jena, A.K. and M.C. Chaturvedi, "Review – The Role of Alloying Elements in the Design of Nickel-Base Superalloys", *Journal of Materials Science*, Vol. 19, pp. 3121-3139, 1984.

8. Holt, R.T. and W. Wallace, "Impurities and Trace Elements in Nickel-Base Superalloys", *International Metals Reviews*, Vol. 21, pp. 1-24, March 1976.

9. Sabol, G.P. and R. Stickler, "Microstructure of Nickel-Based Superalloys", *Physica Status Solidi*, Vol. 35, No. 1, pp. 11-52, 1969.

10. Kotval, P.S., "The Microstructure of Superalloys", *Metallography*, Vol. 1, pp. 251-285, 1969.

11. Sullivan, C.P. and M.J. Donachie, Jr., "Some Effects of Microstructure on the Mechanical Properties of Nickel-Base Superalloys", *Metals Engineering Quarterly*, Vol. 7, No. 1, pp. 36-45, 1967.

12. Porter, D.A. and K.E. Easterling, *Phase Transformations in Metals and Alloys*, Chapman and Hall, 1992.

13. Lifshitz, I.M. and V.V. Sloyozov, "The Kinetics of Precipitation from Supersaturated Solid Solutions", *Journal of Physics and Chemistry of Solids*, Vol.19, No. 1-2, pp.35-50, 1961.

14. Wagner, C., "Theorie der Alterung von Niederschlagen Durch Umlosen (Ostwald-Reifung)", *Zeitschrift für Elektrochemie*, Vol. 65, No. 7-8, pp. 581-591, 1961.

15. Ardell, A.J., "The Effect of Volume Fraction on Particle Coarsening: Theoretical Considerations", *Acta Metallurgica*, Vol. 20, No. 1, pp. 61-71, 1972.

16. Brailsford, A.D. and P. Wynblatt, "Dependence of Ostwald Ripening Kinetics on Particle Volume Fraction", *Acta Metallurgica*, Vol. 27, No. 3, pp. 489-497, 1979.

17. Davies, C.K.L., P. Nash and R.N. Stevens, "Effect of Volume Fraction of Precipitate on Ostwald Ripening", *Acta Metallurgica*, Vol. 28, No. 2, pp. 179-189, 1980.

18. Tsumuraya, K. and Y. Miyata, "Coarsening Models Incorporating Both Diffusion Geometry and Volume Fraction of Particles", *Acta Metallurgica*, Vol. 31, No. 3, pp. 437-452, 1983.

19. Marqusee, J.A. and J. Rose, "Theory of Ostwald Ripening – Competitive Growth and Its Dependence on Volume Fraction", *Journal of Chemical Physics*, Vol. 80, No. 1, pp. 536-543, 1984.

20. Voorhees, P. W. and M.E. Glicksman, “Solution to the Multi-Particle Diffusion Problem with Applications to the Ostwald Ripening – 1. Theory”, *Acta Metallurgica*, Vol. 32, No. 11, pp. 2001-2011, 1984.

21. Voorhees, P. W. and M.E. Glicksman, “Solution to the Multi-Particle Diffusion Problem with Applications to the Ostwald Ripening – 2. Computer Simulations”, *Acta Metallurgica*, Vol. 32, No. 11, pp. 2013-2030, 1984.

22. Henderson, P.J. and M. McLean, “Microstructural Contributions to Friction Stress and Recovery Kinetics During Creep of the Nickel-Base Superalloy IN738C”, *Acta Metallurgica*, Vol. 31, No. 8, pp. 1203-1219, 1983.

23. Balikci, E., A. Raman and R.A. Mirshams, “Influence of Various Heat Treatments on the Microstructure of Polycrystalline IN738LC”, *Metallurgical and Materials Transactions A*, Vol. 28A, pp. 1993-2003, 1997.

24. Safari, J. and S. Nategh, “On the Heat Treatment of Rene-80 Nickel-Base Superalloy”, *Journal of Materials Processing Technology*, Vol. 176, pp. 240-250, 2006.

25. Ricks, R.A., A.J. Porter and R.C. Ecob, “The Growth of γ' Precipitates in Nickel-Base Superalloys”, *Acta Metallurgica*, Vol. 31, pp. 43-53, 1983.

26. Grosdidier, T., A. Hazotte and A. Simon, “Precipitation and Dissolution Processes in γ/γ' Single Crystal Nickel-Based Superalloys”, *Materials Science and Engineering*, Vol. A256, pp. 183-196, 1998.

27. Roy, I., E. Balikci, S. Ibekwe and A. Raman, “Precipitate Growth Activation Energy Requirements in the Duplex Size γ' Distribution in the Superalloy IN738LC”, *Journal of Materials Science*, Vol. 40, pp. 6207-6215, 2005.

28. Ardell, A.J., “An Application of the Theory of Particle Coarsening: The γ' Precipitate in Ni-Al Alloys”, Acta Metallurgica, Vol. 16, pp. 511-516, 1968.

29. Rastoghi, P.K. and A.J. Ardell, "The Coarsening Behavior of the γ' Precipitate in Nickel-Silicon Alloys", *Acta Metallurgica*, Vol. 19, pp. 321-330, 1971.

30. Davies, C.K.L., P. Nash and R.N. Stevens, "The Effect of Volume Fraction of Precipitate on Ostwald Ripening", *Acta Metallurgica*, Vol. 28, pp. 179-189, 1980.

31. Khachaturyan, A.G., S.V. Semenovskaya and J.W. Morris, Jr., "Theoretical Analysis of Strain Induced Shape Changes in Cubic Precipitates During Coarsening", *Acta Metallurgica*, Vol. 36, No. 6, pp. 1563-1572, 1988.

32. Johnson, W.C., T.A. Abinandanan and P.W. Voorhees, "The Coarsening Kinetics of Two Misfitting Particles in an Anisotropic Crystal", *Acta Metallurgica et Materialia*, Vol. 38, No. 7, pp. 1349-1367, 1990.

33. Abinandanan, T.A. and W.C. Johnson, "Coarsening of Elastically Interacting Coherent Particles – I. Theoretical Formulation", *Acta Metallurgica et Materialia*, Vol. 41, No. 1, pp. 17-25, 1993.

34. Abinandanan, T.A. and W.C. Johnson, "Coarsening of Elastically Interacting Coherent Particles – II. Simulations of Preferential Coarsening and Particle Migrations", *Acta Metallurgica et Materialia*, Vol. 41, No. 1, pp. 27-39, 1993.

35. Socrate, S. and D.M. Parks, "Numerical Determination of the Elastic Driving Force for Directional Coarsening in Ni-Superalloys", *Acta Metallurgica et Materialia*, Vol. 41, No. 7, pp. 2185-2209, 1993.

36. Abinandanan, T.A. and W.C. Johnson, "Development of Spatial Correlations During Coarsening", *Materials Science and Engineering*, Vol. B32, pp. 169-176, 1995.

37. Svoboda, J. and P. Lukas, "Modeling of Kinetics of Directional Coarsening in Ni-Superalloys", *Acta Metallurgica*, Vol. 44, No. 6, pp. 2557-2565, 1996.

38. Baldan, A., “Progress in Ostwald Ripening Theories and Their Applications to Nickel-Base Superalloys, Part 1: Ostwald Ripening Theories”, *Journal of Materials Science*, Vol. 37, pp. 2171-2202, 2002.

39. Baldan, A., “Progress in Ostwald Ripening Theories and Their Applications to γ' Precipitates in Nickel-Base Superalloys, Part 2: Nickel Base Superalloys”, *Journal of Materials Science*, Vol. 37, pp. 2379-2405, 2002.

40. Vaithyanathan, V. and L.Q. Chen, “Coarsening of Ordered Intermetallic Precipitates with Coherency Stress”, *Acta Materialia*, Vol. 50, pp. 4061-4073, 2002.

41. Prikhodko, S.V. and A.J. Ardell, “Coarsening of γ' in Ni-Al Alloys Aged Under Uniaxial Compression: I. Early-Stage Kinetics”, *Acta Materialia*, Vol. 51, pp. 5001-5012, 2003.

42. Prikhodko, S.V. and A.J. Ardell, “Coarsening of γ' in Ni-Al Alloys Aged Under Uniaxial Compression: II. Diffusion Under Stress and Retardation of Coarsening Kinetics”, *Acta Materialia*, Vol. 51, pp. 5013-5019, 2003.

43. Prikhodko, S.V. and A.J. Ardell, “Coarsening of γ' in Ni-Al Alloys Aged Under Uniaxial Compression: I. Characterization of the Morphology”, *Acta Materialia*, Vol. 51, pp. 5021-5036, 2003.

44. Ges, A.M., O. Fornaro and H.A. Palacio, “Coarsening Behavior of a Ni-Base Superalloy Under Different Heat Treatment Conditions”, *Materials Science and Engineering A*, Vol. 458, pp. 96-100, 2007.

45. Jinjiang, Y., S. Xiaofeng, Z. Nairen, J. Tao, G. Hengrong and H. Zhuangqi, “Effect of Heat Treatment on Microstructure and Stress Rupture Life of DD32 Single Crystal Ni-Base Superalloy”, *Materials Science and Engineering A*, Vol. 460-461, 2007.

46. Eshelby, J.D., "The Determination of the Elastic Field of an Ellipsoidal Inclusion, and Related Problems", *Proceedings of the Royal Society of London, Series A, Mathematical and Physical Sciences*, Vol. 241, No. 1226, pp. 376-396, 1957.

47. Eshelby, J.D., "The Elastic Field Outside an Ellipsoidal Inclusion", *Proceedings of the Royal Society of London, Series A, Mathematical and Physical Sciences*, Vol. 252, No. 1271, pp. 561-569, 1959.

48. Ardell, A.J., R.B. Nicholson and J.D. Eshelby, "On the Modulated Structure of Aged Ni-Al Alloys", *Acta Metallurgica*, Vol. 14, pp. 1295-1309, 1966.

49. Khachaturyan, A.G., "Some Questions Concerning the Theory of Phase Transformations in Solids", *Soviet Physics-Solid State*, Vol. 8, No. 9, pp. 2163-2168, 1967.

50. Khachaturyan, A.G. and G.A. Shatalov, "Theory of Macroscopic Periodicity for a Phase Transition in the Solid State", *Soviet Physics JETP*, Vol. 29, No.3, pp. 557-561, 1969.

51. Lin, S.C. and T. Mura, "Elastic Fields of Inclusions in Anisotropic Media (II)", *Physica Status Solidi A*, Vol. 15, pp. 281-285, 1973.

52. Mura, T. and P.C. Cheng, "The Elastic Field Outside an Ellipsoidal Inclusion", *Journal of Applied Mechanics*, Vol. 44, No. 4, pp. 591-594, 1977.

53. Mori, T., P.C. Cheng, M. Kato and T. Mura, "Elastic Strain Energies of Precipitates and Periodically Distributed Inclusions in Anisotropic Media", *Acta Metallurgica*, Vol. 26, pp. 1435-1441, 1978.

54. Seitz, E. and D. De Fontaine, "Elastic Interaction Energy Calculations for Guinier-Preston Zones in Al-Cu and Cu-Be", *Acta Metallurgica*, Vol. 26, pp. 1671-1679, 1978.

55. Miyazaki, T., K. Nakamura and H. Mori, "Experimental and Theoretical Investigations on Morphological Changes of γ' Precipitates in Ni-Al Single Crystal during Uniaxial Stress-Annealing", *Journal of Materials Science*, Vol. 14, pp. 1827-1837, 1979.

56. Johnson, W.C. and J.K. Lee, "Elastic Interaction Energy of Two Spherical Precipitates in an Anisotropic Matrix", *Metallurgical Transactions A*, Vol. 10A, pp. 1141-1149, 1979.

57. Yamauchi, H. and D. De Fontaine, "Elastic Interaction of Defect Clusters with Arbitrary Strain Fields in an Anisotropic Continuum", *Acta Metallurgica*, Vol. 27, pp. 763-776, 1979.

58. Miyazaki, T., H. Imamura and T. Kozakai, "The Formation of γ' Precipitate Doublets in Ni-Al Alloys and their Energetic Stability", *Materials Science and Engineering*, Vol. 54, pp. 9-15, 1982.

59. Doi, M., T. Miyazaki and T. Wakatsuki, "The Effect of Elastic Interaction Energy on the Morphology of γ' Precipitates in Nickel-Based Alloys", *Materials Science and Engineering*, Vol. 67, pp. 247-253, 1984.

60. Johnson, W.C., "On the Elastic Stabilization of Precipitates Against Coarsening under Applied Load", *Acta Metallurgica*, Vol. 32, No. 3, pp. 465-475, 1984.

61. Johnson, W.C., "Elastic Interaction and Stability of Misfitting Cuboidal Inhomogeneities", *Journal of Applied Physics*, Vol. 61, No. 4, pp. 1610-1619, 1987.

62. Khachaturyan, A.G., S.V. Semenovskaya and J.W. Morris, Jr., "Theoretical Analysis of Strain-Induced Shape Changes in Cubic Precipitates during Coarsening", *Acta Metallurgica*, Vol. 36, No. 6, pp. 1563-1572, 1988.

63. Doi, M., “Coarsening Behavior of Coherent Precipitates in Elastically Constrained Systems – with Particular Emphasis on Gamma-Prime Precipitates in Nickel-Base Alloys”, *Materials Transactions, JIM*, Vol. 33, No. 7, pp. 637-649, 1992.

64. Bieber, C.G. and J.J. Galka, “Cast Nickel-Base Alloy”, United States Patent Office, No. 3,459,545, August 1969.

65. Balikci, E. and A. Raman, “Characteristics of the γ' Precipitates at High Temperatures in Ni-Base Polycrystalline Superalloy IN738LC”, *Journal of Materials Science*, Vol. 35, No. 14, pp. 3593-3597, 2000.

66. Frenz, H., J. Meersmann, J. Ziebs, H.J. Kühn, R. Sievert and J. Olschewski, “High Temperature Behavior of IN738LC under Isothermal and Thermo-Mechanical Cyclic Loading”, *Materials Science and Engineering A*, Vol. 230, No. 1-2, pp. 49-57, 1997.

67. Balikci, E., *Microstructure Evolution and Its Influence on Thermal Expansion and Tensile of the Superalloy IN738LC at High Temperatures*, Ph.D. Thesis, Louisiana State University, 1998.

68. Balikci, E., R.A. Mirshams and A. Raman, “Microstructure Evolution in Polycrystalline IN738LC in the Range 1120 to 1250°C”, *Zeitschrift für Metallkunde*, Vol. 90, No. 2, pp. 132-140, 1999.

69. Dwarapureddy, K., E. Balikci, S. Ibekwe, and A. Raman, “Activation energy for growth in single size distribution and the dissolution features of γ' precipitates in the superalloy IN738LC”, *Journal of Materials Science*, Vol. 43, No. 6, pp. 1802-1810, 2008.

70. Prikhodko, S.V. and A.J. Ardell, “Coarsening of γ' in Ni-Al Alloys Aged under Uniaxial Compression: Characterization of the Morphology”, *Acta Materialia*, Vol. 51, pp. 5021-5036, 2003.

71. Balikci, E., R.A. Mirshams and A. Raman, “Tensile Strengthening in the Nickel-Base Superalloy IN738LC”, *Journal of Materials Engineering and Performance*, Vol. 9, No. 3, pp. 324-329, 2000.